Geological Magazine

www.cambridge.org/geo

Late Jurassic – earliest Cretaceous prolonged shelf dysoxic–anoxic event and its possible causes

MA Rogov[1,2], EV Shchepetova[1] and VA Zakharov[1]

[1]Geological Institute of RAS, Pyzhevski lane 7/1, Moscow 119017, Russia and [2]Saint-Petersburg State University, Universitetskaya nab. 7/9, Saint Petersburg 199034, Russia

Original Article

Cite this article: Rogov MA, Shchepetova EV, and Zakharov VA (2020) Late Jurassic – earliest Cretaceous prolonged shelf dysoxic–anoxic event and its possible causes. *Geological Magazine* **157**: 1622–1642. https://doi.org/10.1017/S001675682000076X

Received: 13 February 2019
Revised: 25 June 2020
Accepted: 29 June 2020
First published online: 19 August 2020

Keywords:
black shales; oceanic anoxic events (OAEs); Jurassic; Cretaceous; shelf dysoxic–anoxic event (SDAE); nannoplankton; radiolarians

Author for correspondence: MA Rogov, Email: russianjurassic@gmail.com

Abstract

The Late Jurassic – earliest Cretaceous time interval was characterized by a widespread distribution of dysoxic–anoxic environments in temperate- and high-latitude epicontinental seas, which could be defined as a shelf dysoxic–anoxic event (SDAE). In contrast to black shales related to oceanic anoxic events, deposits generated by the SDAE were especially common in shelf sites in the Northern Hemisphere. The onset and termination of the SDAE was strongly diachronous across different regions. The SDAE was not associated with significant disturbances of the carbon cycle. Deposition of organic-carbon-rich sediment and the existence of dysoxic–anoxic conditions during the SDAE lasted up to *c.* 20 Ma, but this event did not cause any remarkable biotic extinction. Temperate- and high-latitude black shale occurrences across the Jurassic–Cretaceous boundary have been reviewed. Two patterns of black shale deposition during the SDAE are recognized: (1) Subboreal type, with numerous thin black shale beds, bounded by sediments with very low total organic carbon (TOC) values; and (2) Boreal type, distinguished by predominantly thick black shale successions showing high TOC values and prolonged anoxic–dysoxic conditions. These types appear to be unrelated to differences in accommodation space, and can be clearly recognized irrespective of the thickness of shale-bearing units. Black shales in high-latitude areas in the Southern Hemisphere strongly resemble Boreal types of black shale by their mode of occurrence. The causes of this SDAE are linked to long-term warming and changes in oceanic circulation. Additionally, the long-term disturbance of planktonic communities may have triggered overall increased productivity in anoxia-prone environments.

1. Introduction

Oceanic anoxic events (OAEs) are attracting much attention due to their impact on the development of life, and the burial of organic carbon in marine sediments leading to the formation of black to organic-rich shales of high economical value. During the last decades, numerous studies of OAEs across the world have revealed some of their distinctive features. OAEs were widely distributed across both oceanic and shelf basins, and were associated with perturbations of the global carbon cycle (Jenkyns, 2010). They are generally of short duration, lasting some tens to hundreds of thousand years. The onset of typical OAEs is nearly synchronous across different basins, and associated excursions in carbon isotope values can also be traced in non-marine successions. OAEs are also associated with elevated global temperatures, as well as significant faunal turnovers and sometimes extinctions (Jenkyns, 1999).

In addition to typical OAEs, other intervals characterized by widespread black shale distribution are known of. In particular, the Upper Jurassic – lowermost Cretaceous interval stands out as one of the most important. It can be traced across multiple middle- to high-latitude basins and sub-basins from NW Europe to the Polish Lowlands and the European part of Russia, and from the North Sea and East Greenland to Western and Northern Siberia, Alaska and Arctic Canada. Significant differences from typical OAEs preclude this period from being identified as a Late Jurassic anoxic event (Nozaki *et al.* 2013; Arora *et al.* 2015; Carmeille *et al.* 2020) or an Oxfordian–Kimmeridgian OAE (Trabucho-Alexandre *et al.* 2012; Martinez & Dera, 2015). Here we propose to recognize the Late Jurassic – earliest Cretaceous shelf dysoxic–anoxic event (SDAE), named in such a manner because it influenced shelf environments, mainly in high latitudes. It is characterized by the following set of key features.

(1) Latest Jurassic – earliest Cretaceous black shales are very rare in low-latitude areas and oceanic sites, but very widely distributed in Boreal shelves (and also known from the high-latitude sites of the Southern Hemisphere).
(2) The onset and termination of this SDAE were strongly diachronous within laterally different palaeobasins and sometimes inside the same basin.

CAMBRIDGE UNIVERSITY PRESS

(3) The deposition of finely laminated organic-carbon-rich sediments and, accordingly, the existence of associated dysoxic–anoxic environments lasted for several million years (up to *c.* 20 Ma; see Georgiev *et al.* 2017).
(4) There is no evidence for any significant perturbations in the global carbon cycle during the SDAE.
(5) The long-term development of dysoxic–anoxic conditions near the sediment–water interface strongly affected benthic faunas, but did not lead to any remarkable extinction events.

This paper is focused on an analysis of the distribution of black shales near the Jurassic–Cretaceous (J/K) boundary. The term 'black shales' follows the definition by Tyson (1987): "dark-coloured, fine grained mudrocks having the sedimentological, palaeoecological and geochemical characteristics associated with deposition under oxygen-deficient or oxygen-free bottom waters". Additionally, Tyson (1987) emphasized the high content of total organic carbon (TOC usually more than 1%; see also Arthur & Sageman, 1994), and a predominantly marine origin of the organic matter (OM). Black shales are usually well-laminated due to a general lack of bioturbation (Savrda & Bottjer, 1986).

An additional comment should be made concerning the stage names used in this paper and Boreal–Tethyan correlation (Fig. 1). Significant faunal provincialism near to the J/K boundary (Enay, 1972; Rawson, 1973; Remane, 1991; Cecca, 1999; Zakharov & Rogov, 2003; Wimbledon, 2008) has led to continuous use of independent stages for Tethyan (internationally accepted Tithonian and Berriasian stages) and Boreal (Volgian and Ryazanian stages) regions. Although the base of the Volgian stage is coinciding with the base of the Tithonian stage (Rogov, 2004, 2010) and top of the Ryazanian stage lies close to the top of the Berriasian stage (Baraboshkin, 2004), the Volgian–Ryazanian boundary corresponds to a level somewhere within the lower Berriasian stage (Houša *et al.* 2007; Bragin *et al.* 2013). It should also be noted that although the Volgian and Tithonian ammonite zones can be correlated (Rogov, 2014), the use of the Volgian and Ryazanian stages is preferred for the Boreal regions in this paper as all boundaries of these stages are clearly traced across the Boreal areas (Baraboshkin, 2004; Rogov & Zakharov, 2009), while substages of the Tithonian and Berriasian stages cannot be recognized here.

2. Late Jurassic – earliest Cretaceous black shales in space and time

The wide distribution of Late Jurassic – earliest Cretaceous black shales in temperate- and high-latitude areas of the Northern Hemisphere is well-known, especially due to the high source-rock potential of these rocks. However, there exist relatively few papers summarizing the occurrences of these black shales (cf. Braduchan *et al.* 1989; Wignall, 1990; Leith *et al.* 1992); we therefore provide a brief review of black shale occurrences. We also consider low-latitude Subboreal black shales (such as those from England and northern France), as both the mode of occurrence and faunal contents of these black shales show similarities with those of northern high-latitudes.

Two different patterns of black shale deposition during the Late Jurassic – earliest Cretaceous SDAE can be recognized. (a) Type 1 are Subboreal (Kimmeridge Clay Formation) and are characterized by intercalations of black shales and typical shallow-water mudstones, marlstones, sandstones, etc; the sands, marls and muds were deposited in well-oxygenated environments. This type of black shale is mainly restricted to relatively low latitudes (35–50° N). (b) Type 2 are Boreal (Bazhenovo Formation of the Western Siberia) and characterized by thick, monotonous black shale units of variable thickness that were deposited in anoxic–dysoxic environments of long duration. Type 2 black shales are more typical of high palaeolatitudes (Fig. 2; online Supplementary Table S1, available at http://journals.cambridge.org/geo).

Type 1 black shales of the Subboreal type are especially well-studied in the type area of the famous Kimmeridge Clay Formation (Figs 2, 3a). These black shales span the upper Kimmeridgian – lowermost middle Volgian interval (Cope, 1967, 1978; Callomon & Cope, 1971; Morgans-Bell *et al.* 2001; Gallois, 2004, 2011). Numerous black shale bands are exposed along the Dorset and Yorkshire coasts, penetrated by many exploration or scientific boreholes, and further expanded offshore to the North Sea (Gallois, 2004). These black shales, characterized by specific dysoxic–anoxic benthic assemblages (Wignall, 1990; Oschmann, 1994), are intercalated with mudstone–marlstone beds indicating well-oxygenated near-bottom conditions. It should be noted, however, that not all black shale bands are clearly associated with prominent anoxia, but additional factors controlling black shale deposition (enhanced bioproductivity, high sediment accumulation rates and rapid burial) are also important (Tribovillard *et al.* 2005). Fossil assemblages of the Kimmeridge Clay Formation (including black shale bands) are especially diverse and include some unique records of both invertebrates and vertebrates (Etches & Clarke, 1999; Gallois, 2004). The oxygen-depleted environments clearly favoured preservation of organic material. Total pyrolysed and residual organic carbon (TOC, %) values in the black shales vary from 2–4% to 10–12%, sometimes reaching 13–15% or 28–32% (Scotchman, 1991; Sælen *et al.* 2000; Morgans-Bell *et al.* 2001). RockEval Pyrolysis data and the distribution of the hydrogen index of kerogen (HI = S2/TOC, where S2: the amount of hydrocarbons from the thermal cracking of insoluble OM, measured in mg HC g^{-1}) with the temperature of the maximum rate of hydrocarbon generation occurring in a kerogen sample during pyrolysis (measured at the top of the S2 peak; T_{max}) (Fig. 4a) determine mainly 'immature' kerogen of Type II and III, which indicates a mixture of marine and terrestrial OM present in variable proportions (Scotchman, 1991; Sælen *et al.* 2000). Increased TOC values in the black shales typically coincide with elevated HI (Fig. 4a), indicating an increase in the marine OM contribution to the kerogen composition. In northern Scotland (Isle of Skye) the deposition of black shales began earlier, and here black shales of the Subboreal type are known from the Oxfordian – lower Kimmeridgian Staffin Shale Formation (Nunn *et al.* 2009). TOC values here range from 0.2 to 9.2 wt% with values increasing up the sequence, although highest values were reported from the lower Oxfordian substage. RockEval pyrolysis indicated mainly Type III kerogen, while *c.* 10% of samples indicated Type II kerogen (Fig. 2).

Similar occurrences and stratigraphic ranges of black shales are known from the opposite coast of the English Channel, that is, in northern France (Herbin *et al.* 1995; Proust *et al.* 1995; Samson *et al.* 1996; Gallois, 2005). However, the duration of black shale deposition is reduced and the number of elementary black shale bands here are fewer when compared with coeval strata in Dorset (Fig. 2). Black shale bands in this region, although bounded by TOC-depleted beds, are sometimes relatively thick (Geyssant *et al.* 1993). According to Tribovillard *et al.* (2001) and Hatem *et al.* (2018), the TOC values in the black shales falls in the range 2–7% and sometimes 9%. Type II–III kerogen is represented mainly by amorphous OM interpreted as marine biomass degraded as a result of selective oxidation of metabolizable

https://doi.org/10.1017/S001675682000076X Published online by Cambridge University Press

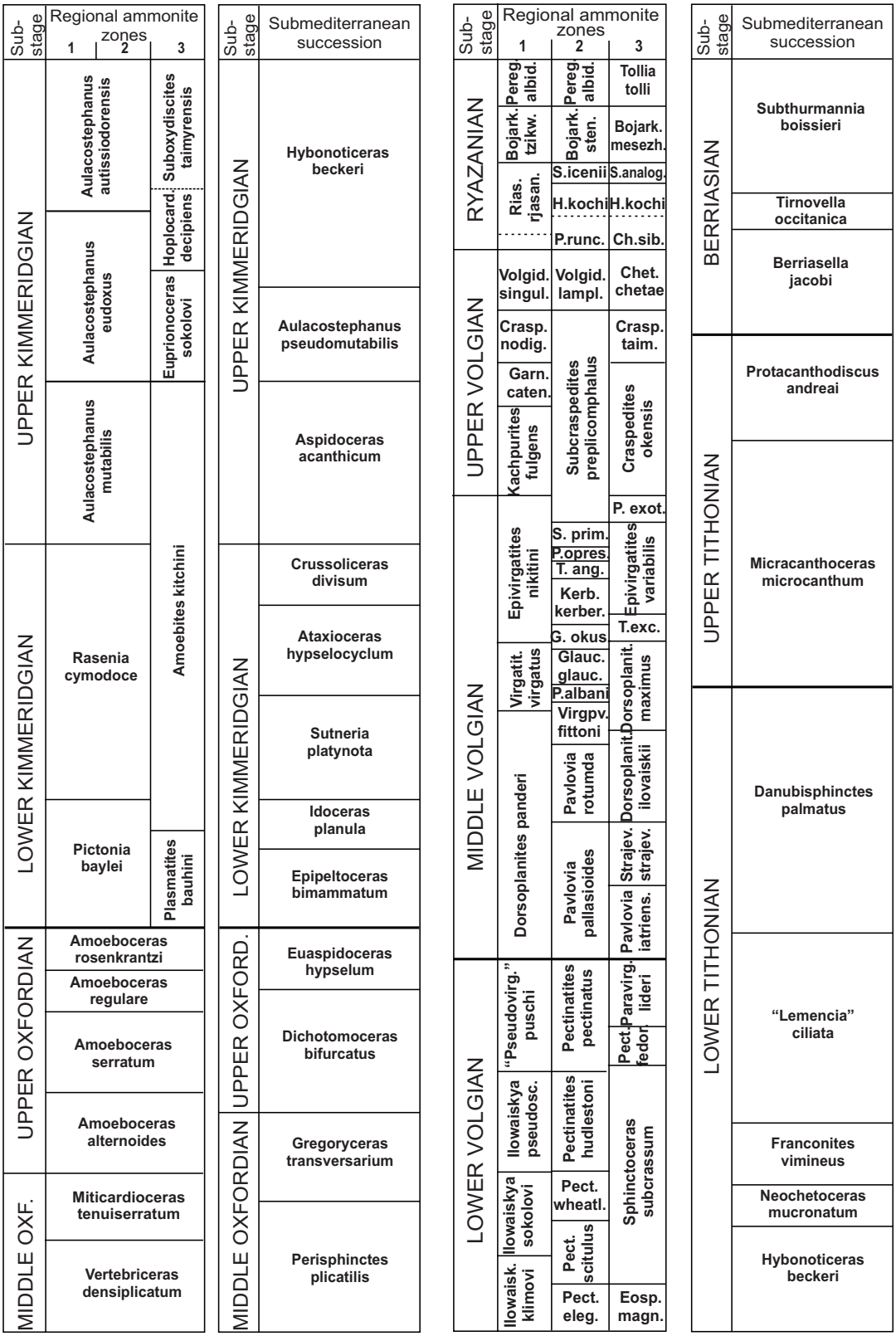

Fig. 1. Correlation of the regional ammonite biostratigraphic scales for the Oxfordian–Berriasian period. Boreal zonal successions are provided for 3 regions: (1) the Russian Platform; (2) England and (3) Northern Siberia. Correlation of the Volgian part of the succession is after Rogov & Zakharov (2009), with minor corrections.

components, and partly by incorporation of reduced inorganic sulphur into lipids (Hatem *et al.* 2018).

Black shales belonging to the Subboreal type can also be found in the Polish Lowlands. Both lithologies and fossil contents of the Kimmeridgian and lower Volgian deposits here are very close to those of the Volga Basin (Rogov, 2010), and the measured TOC concentrations (0.2–9.2 wt%) from the central–eastern part of the Łódź Synclinorium are comparable to those of the

https://doi.org/10.1017/S001675682000076X Published online by Cambridge University Press

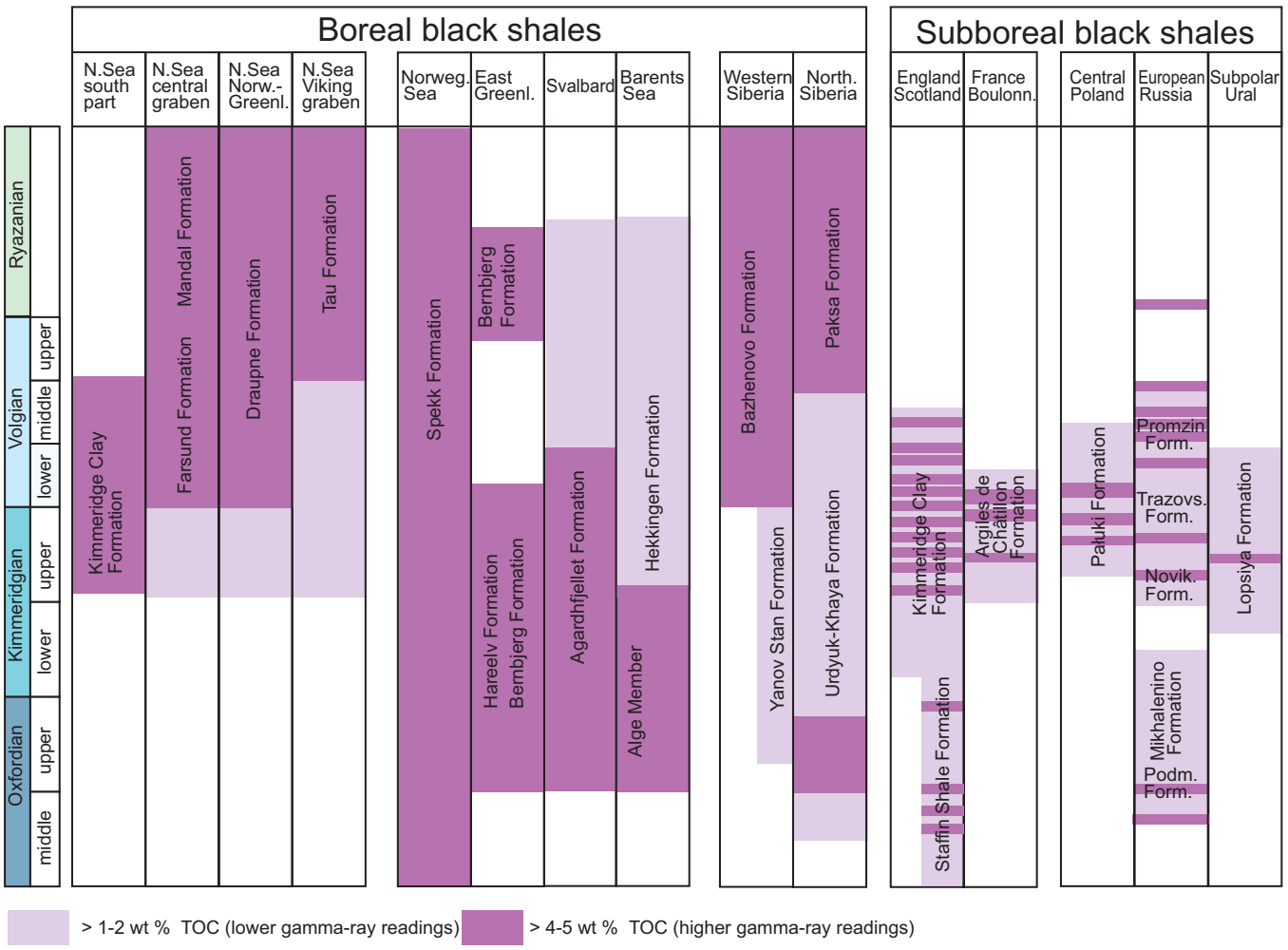

Fig. 2. Black shale distribution across the J/K boundary in the Boreal areas of the Northern Hemisphere. N – North; Norw – Norway; Norweg – Norwegian; Greenl – Greenland; North – Northern; Boulonn – Boulonnais; Form – Formation; Novik – Novikovka; Podm – Podmoskovie; Trazovs – Trazovskaya; Promzin – Promzinskaya; for data source see text.

Kimmeridge Clay facies of NW Europe (Wierzbowski & Wierzbowski, 2019). The geochemical studies of the Upper Jurassic deposits in Central Poland (Socha & Makos, 2016; Więcław, 2016; Wierzbowski & Wierzbowski, 2019) indicate high potential for hydrocarbon generation in the dark-grey shaly calcareous claystones, interlayered with light-grey mudstones, marls or marly limestones of the upper Kimeridgian – middle Volgian Pałuki Formation (100–125 m in thickness). Dark shaly claystones with TOC values of *c.* 3–6% on average, sometimes reaching 9–11%, contain mainly Type II kerogen, sometimes with HI reaching 500–700 (Socha & Makos, 2016; Więcław, 2016; Wierzbowski & Wierzbowski, 2019). However, the T_{max} values (423–439°C) indicate the low thermal maturity of the rocks in the Pałuki Formation (Wierzbowski & Wierzbowski, 2019).

Black shales are especially widely distributed on the Russian Platform (Braduchan *et al.* 1989; Zakharov *et al.* 2017) but can be subdivided into three parts based on their stratigraphic ranges (Figs 2, 5a, b).

(1) The lower interval corresponds to the uppermost middle Oxfordian – uppermost lower Volgian deposits and is characterized by very few black shale bands, with TOC values varying from 4–6% to 16–17%. These black shales can be traced over distances from a few kilometres to *c.* 1000 km. Black shales are highly enriched in amorphous OM and commonly contain fine plant detritus (Bushnev *et al.* 2006; Gavrilov *et al.* 2014). RockEval parameters HI and T_{max} (Hantzpergue *et al.* 1998; Shchepetova & Rogov, 2013, 2016; Gavrilov *et al.* 2014; Ilyasov *et al.* 2018) indicate that the Type II and III kerogen is of low thermal maturity (Fig. 4b), originating largely from marine microplankton with an admixture of terrestrial plant components. Fossil contents of these black shales are very different from one band to another. For example, black shale bands in the basal part of the upper Oxfordian substage (i.e. Głowniak *et al.* 2010) are characterized by relatively diverse ammonites, coleoids and benthonic fossils, which are usually overcrowding bedding planes (Fig. 6f–g). On the other hand, black shale bands in the upper Kimmeridgian Mutabilis Zone typically contain very few ammonites and sometimes bivalve (*Aulacomyella*) and gastropod accumulations (Fig. 6h).

(2) The middle interval belongs to the middle Volgian Dorsoplanites panderi Zone (Rogov, 2013). It is characterized by a succession with well-defined decimetre- to metre-scale cyclicity, formed by alternations of black shales (TOC up to 25%) and calcareous clays or mudstones. Volgian black shale (so-called Kashpir Oil Shale, according to Ribouleau *et al.* 2001) developed in a wide area extending from the Caspian to Pechora seas. Although the thickness of this sequence varies from a few metres on the midlands of Russia to a hundred metres in the northern slope of the

https://doi.org/10.1017/S001675682000076X Published online by Cambridge University Press

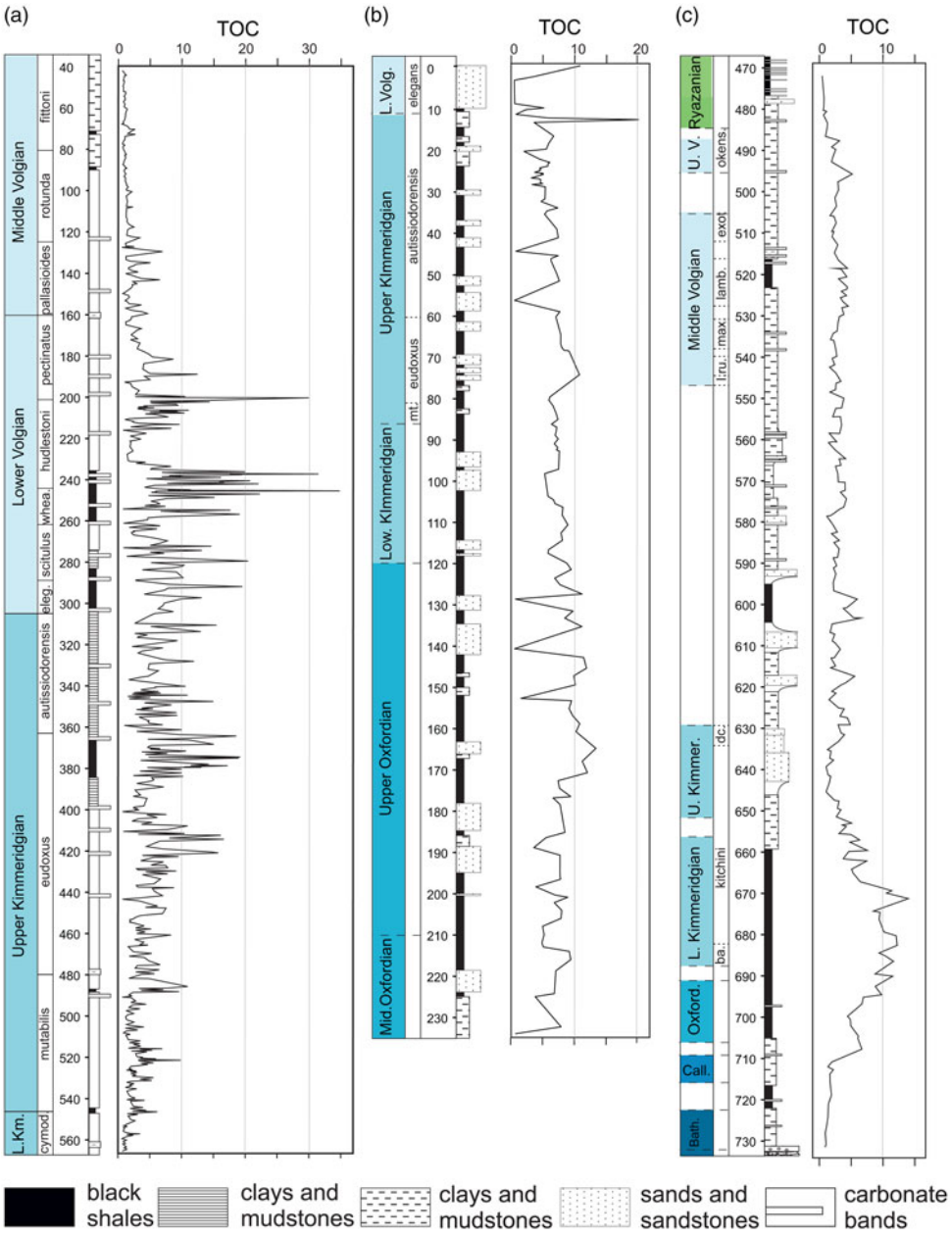

Fig. 3. Typical lithological logs, TOC values, thickness and stratigraphic distribution of black shales belonging to SDAE (western Europe). (a) Swanworth Quarry 1 borehole, England (Morgans-Bell *et al.* 2001); (b) Blokelv-1 borehole, Jameson Land, East Greenland (Bojesen-Koefoed *et al.* 2018; age after Alsen & Piasecki, 2018); and (c) DH2 and DH5R boreholes, Spitsbergen (Koevoets *et al.* 2016, 2019; age after Rogov, unpubl. data). Abbreviations: ba. – bayi; Bath. – Bathonian; Call. – Callovian; cymod. – cymodoce; dc. – decipiens; eleg. – elegans; exot – exoticus; I – iatriensis; Km., Kimmer. – Kimmeridgian; L., Low. – Lower; lamb. – lambecki; L.Volg. – Lower Volgian; max. – maximus; Mid. – Middle; mt. – mutabilis; okens. – okensis; Oxford. – Oxfordian; ru. – Rugosa; U. – Upper; U. V. – Upper Volgian; Volg. – Volgian; whea. – wheatleyensis.

Caspian depression (Fig. 5a, b), and the thickness of individual black shale bands changes from one site to other, the general cyclic structure of this black shale unit remains nearly constant throughout the whole Russian Platform area (Strachoff, 1934; Shchepetova, 2009; see Figs 5a, b, 7a). Kerogen in the Volgian black shales shows a low degree of thermal evolution, as determined by the range of $T_{max} < 435$°C derived from RockEval Pyrolysis (Fig. 4b). Most of these shales are characterized by TOC values > 10%; a high hydrogen index (HI) corresponds mainly to a Type II kerogen, indicating predominance of marine OM, and sometimes to a Type I kerogen, resulting from the accumulation of the most resistant organic components. The middle Volgian black shales are especially rich in ammonites, and can be easily observed in borehole sections, as well as a diverse bivalve fauna dominated by common *Buchia* or *Inoceramus*, gastropods, brachiopods, echinoderms and diverse marine vertebrates. In contrast to many other examples of the SDAE black shales, these beds are also characterized by relatively diverse and abundant benthic fossils (i.e. Strachoff, 1934; Vischnevskaya *et al.* 1999; Fig. 6i). Benthic taxa are usually represented by numerous juveniles in death assemblages related to anoxic events (Vischnevskaya *et al.* 1999; Turov, 2000). Northwards from the middle Volga basin benthic faunal diversity in these black shales drastically decrease, and only *Buchia* and *Inoceramus* usually occur within black shale beds. Remains of coleoid molluscs (i.e. Rogov & Bizikov, 2006) and marine reptiles, especially ichthyosaurs (Zverkov & Efimov, 2019), are also very typical here.

(3) The upper interval is represented by two occurrences of black shale beds corresponding to the upper middle Volgian and lower Ryazanian substages, each known from only a single locality in Central Russia. Very thin (decimetre-scale) black shale horizons, highly enriched in marine organic carbon (TOC up to 16–40%, HI up to 278–444; Fig. 4b) are present within the sandy shallow-water upper middle Volgian – Ryazanian succession

https://doi.org/10.1017/S001675682000076X Published online by Cambridge University Press

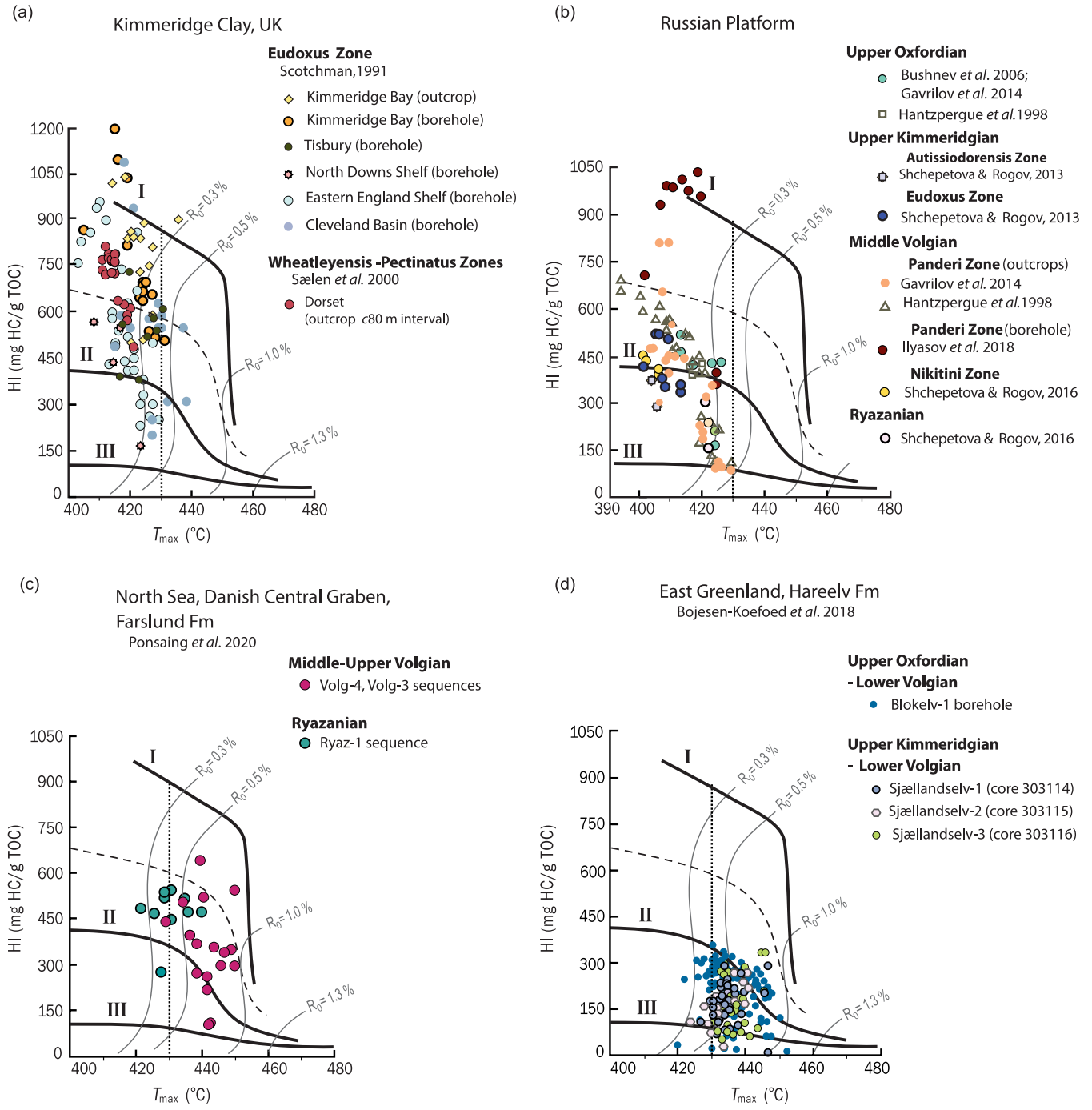

Fig. 4. (a–d) Hydrogen index (HI) versus pyrolysis T_{max} diagrams, showing kerogen type and thermal maturity (after Delvaux *et al.* 1990; Tyson, 1995) of Subboreal and Boreal black shales of Europe. Dashed curve distinguishes kerogen of Type II (marine) and mixed Type II–III (marine and terrestrial). Dotted vertical line (T_{max} = 430°C) subdivides immature and mature kerogen. R_o, vitrinite reflectance.

(6–7 m) (Rogov *et al.* 2015). The upper middle Volgian black shale is characterized by ammonites, indicating the Epivirgatites nikitini Zone. In contrast, the Ryazanian shales are nearly barren of macrofossils and their age assignments are based on their relative stratigraphic position and a single ammonite record (Rogov *et al.* 2015). Black shales belonging to the third interval are characterized by being bounded by sandstone units, not by mudstones (Fig. 7b).

Further eastwards, black shales of the Subboreal type are known from the eastern slope of the Subpolar Urals (Fig. 2). Here, a single band of marine black shale with TOC 12–13%, HI 278–446 and T_{max} 408–420°C is recorded in the upper Kimmeridgian substage (Zakharov *et al.* 2005). It is characterized by a low-diversity molluscan assemblage consisting of cardioceratid ammonites and numerous *Meleagrinella* bivalves (Zakharov *et al.* 2005). This black shale band was previously ascribed to the Mutabilis Zone (Zakharov *et al.* 2005) but, because of the presence of *Aulacostephanus* species (indicative of the Eudoxus Zone in the underlying bed), these black shales were ascribed here to the lower Eudoxus Zone.

https://doi.org/10.1017/S001675682000076X Published online by Cambridge University Press

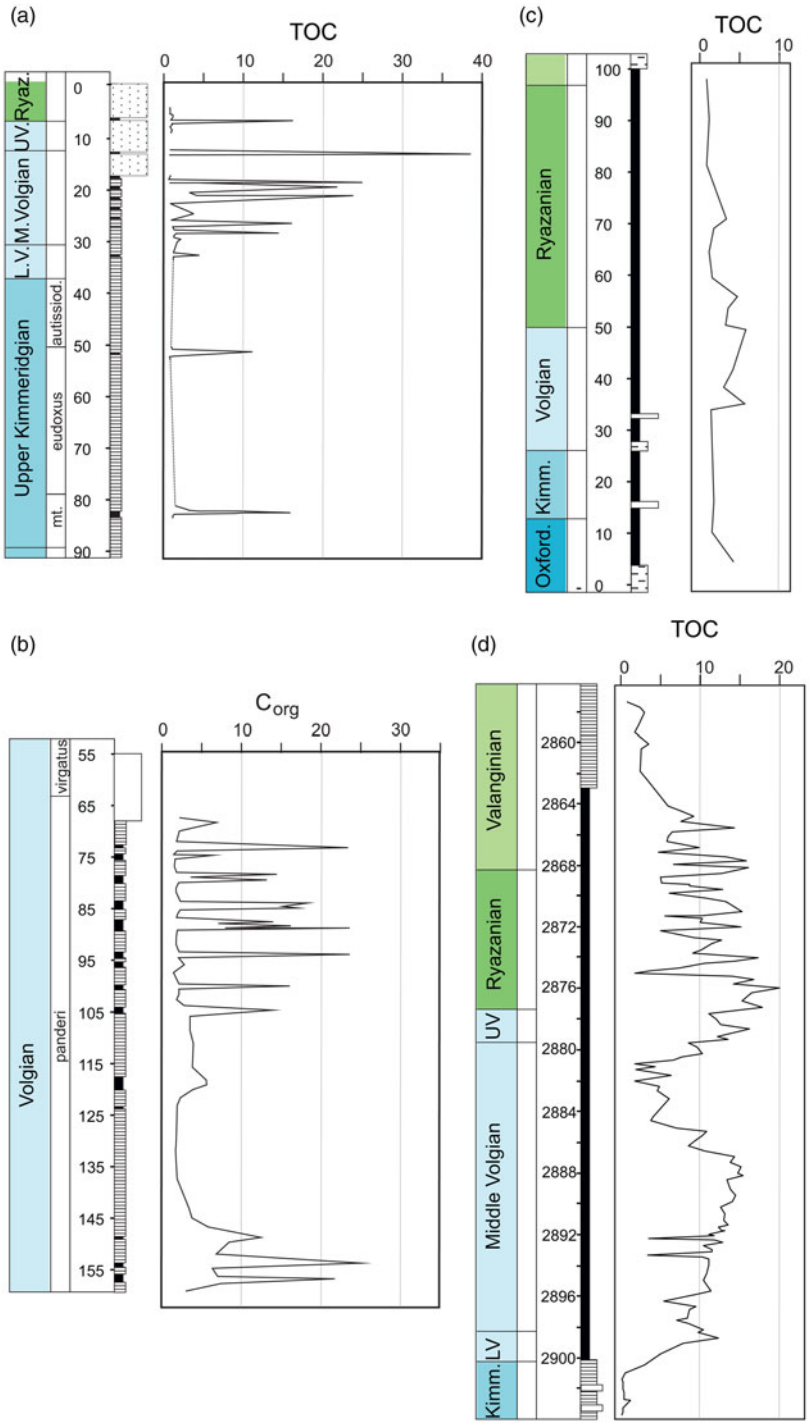

Fig. 5. Typical lithological logs, TOC values, thickness and stratigraphic distribution of black shales belonging to SDAE (eastern Europe and Siberia). (a) Gorodischi, Memei and Kashpir, composite, Volga area, Central Russia (Hantzpergue *et al.* 1998; Rogov, 2010, 2013; Gavrilov *et al.* 2014); (b) borehole 559, Samara region, Central Russia (Kulyova *et al.* 2004); (c) Cape Urdyuk-Khaya, Nordvik peninsula, Northern Siberia (Kashirtsev *et al.* 2018); and (d) borehole no. 6, Western Siberia (Panchenko *et al.* 2015, 2016). autissiod. – autissiodorensis; Kimm. – Kimmeridgian; L., Low. – Lower; LV, L.V. – Lower Volgian; Mid. – Middle; mt. – mutabilis; Oxford. – Oxfordian; U. – Upper; UV – Upper Volgian. For legend see Figure 3.

All aforementioned black shale occurrences of the Subboreal type are characterized by variable vertical TOC profiles, caused by alternation of the black shales with clayey or sandy beds characterized by very low TOC values (Figs 2, 3a, 5a, c). All basins and sub-basins show strongly diachronous onset and termination of the black shale deposition. The occurrences of individual black shale beds or members have significantly changed in space and time: some of the black shale bands are known from a single locality only, while others cover millions of square kilometres. Irrespective of such patchy distribution, individual black shale beds are sometimes characterized by very high TOC values, up to *c.* 30–40% (Fig. 2). Taking into account strongly irregular black shale records, it is not surprising that their occurrences are not associated with any carbon isotope excursions or faunal turnovers (except local turnovers influenced by local environmental perturbations). Cyclicity in the Subboreal black shale could be caused by short-term climate oscillations associated with Milankovich cycles. A very similar type of cyclicity was described in the Lower Cretaceous strata of England and northern Germany (Mutterlose & Ruffell, 1999). Here, the numerous thin pale beds of mudstone with Tethyan fauna, likely indicating surface waters depleted in nutrients, were formed during periods with warm arid

https://doi.org/10.1017/S001675682000076X Published online by Cambridge University Press

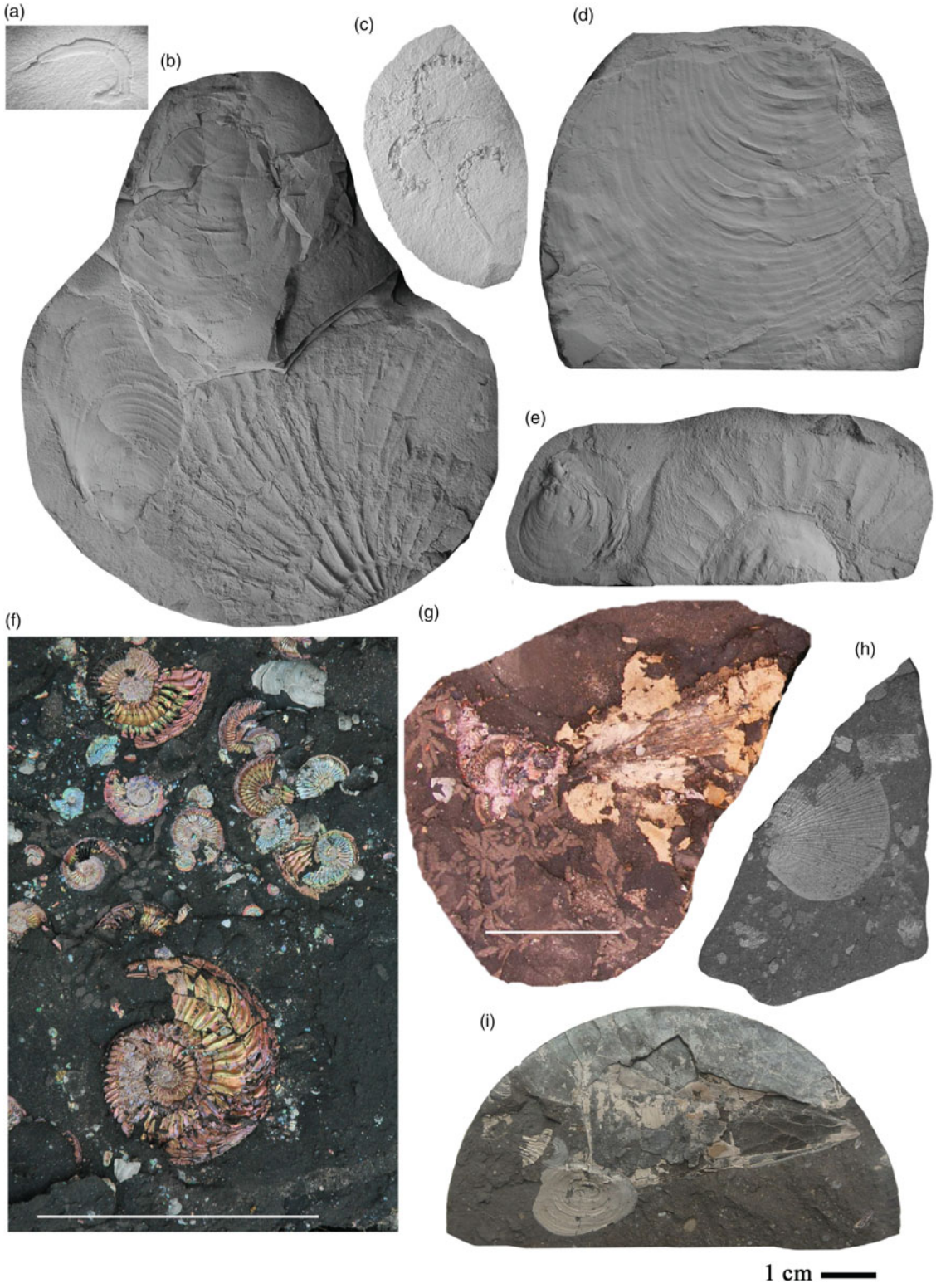

Fig. 6. Typical fossils encountered in Upper Jurassic black shales in Russia. (a, c) Megaonychites, coleoid hooks from the Volgian Stage of Western Siberia; (b, e) Ammonites associated with *Buchia* bivalves and oyster; (e) in the ammonite umbilical region, Volgian Stage of Western Siberia; (d) *Inoceramus* from the Bazhenovo Formation of Western Siberia; (f) Upper Oxfordian black shales showing typical accumulation of juvenile and mature ammonite shells, occasional bivalves and shell debris; Mikhalenino section, Kostroma region, Russia; (g) Fossilized soft tissue remains of the fin and part of the body of coleoid mollusc (age and locality as for (f)); (h) Numerous complete and disarticulated shells of planktonic bivalve *Aulacomyella*, Upper Kimmeridgian, Memei section, Middle Volga area, Russia; (i) Coleoid *Acanthoteuthis* (in the central part of the figure), piece of big-sized inoceramid bivalve (in the top), shell debris and limped gastropod (below coleoid), Middle Volgian of well 559, Samara region, Russia. Scale bar for (f, g) 5 cm; scale bar for other specimens is 1 cm (see lower right corner of the figure).

https://doi.org/10.1017/S001675682000076X Published online by Cambridge University Press

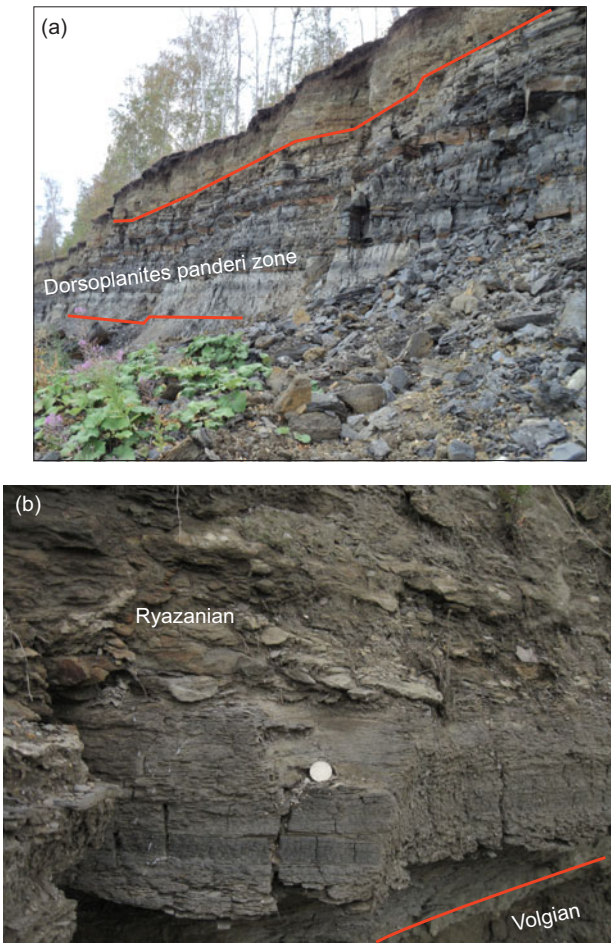

Fig. 7. Black shales of the Subboreal type. (a) Middle Volgian black shales in the Gorodischi section (middle Volga area, Russia). Thickness of black shale member is *c.* 6 m (photograph by MA Rogov). (b) Ryazanian black shales of the Subboreal type embedded between two sandy units in the Kashpir section (middle Volga area, Russia). Diameter of a coin *c.* 2 cm (photograph by SV Maleonkina).

climate while the dark mudstone layers, with a dominantly Boreal fauna, were deposited under cooler-water conditions, rich in nutrients. Although calcareous nannofossils are poorly preserved in black shales due to diagenetic overprint (e.g. in the middle Volgian black shales of the Volga area; see Ruffell *et al.* 2002), ammonite data at least partially support cooler environments during deposition of the dark shale beds. The well-traced black-shale-bearing interval near the top of the Kimmeridgian Eudoxus Zone is commonly overcrowded by Boreal cardioceratids *Nannocardioceras*, while the overlying grey mudstone beds of the base of the Autissiodorensis Zone are usually characterized by numerous Tethyan aspidoceratids both on the Russian Platform and in England (Rogov, 2010). However, the changes in ammonite assemblages of the middle Volgian Panderi zone rather show a gradual warming through time, with increasing Subboreal and/or Boreal ammonite ratios within both the black shales and grey clays (Rogov, 2013).

High-latitude black shale deposits, referred to here as Boreal type (Fig. 2), have been the focus of numerous integrated studies over the past decades. Black shales of the Boreal type are very common in the Arctic, ranging from the North Sea (Vollset & Doré, 1984; Cornford, 1998), East Greenland (Stemmerik *et al.* 1998; Alsgaard *et al.* 2003; Bojesen-Koefoed *et al.* 2018) through Norwegian and Barents sea basins (Dalland *et al.* 1988; Mutterlose *et al.* 2003; Langrock & Stein, 2004; Georgiev *et al.* 2017) to Spitsbergen (Dypvik, 1985; Koevoets *et al.* 2018*a*, *b*), and further E-wards via the Russian part of the Barents Sea shelf, South Kara basin and the Western Siberian depression (Braduchan *et al.* 1986; Ryzhkova *et al.* 2018) to the Yenissei–Khatanga depression (Zakharov *et al.* 2014; Kashirtsev *et al.* 2018) and the Lena River lower reaches in the north (Rogov *et al.* 2011). Eastwards from the Lena River basin, Upper Jurassic successions (sometimes extremely thick, up to 5–6 km thickness) are characterized by the common presence of volcanic rocks, including tuffs and lava flows. Upper Jurassic – lowermost Cretaceous black shales appear in Alaska and the Arctic Canada (Leith *et al.* 1992).

Black shales are inherent constituents of the Late Jurassic – Early Cretaceous formations of the North Sea Graben Province. Thick accumulations of moderately organic carbon-rich shale commonly include extended intervals (from tens to several hundred metres) represented by dark-olive-grey fissile shales, enriched in marine organic carbon up to 5–6% in average, in some cases to 8 to 12–15% (Miller, 1990; Cornford, 1994, 1998). They are also known as 'hot shale' due to the strong natural gamma-ray response (Miller, 1990; Clark *et al.* 1993; Cornford, 1994, 1998; Underhill, 1998; Gautier, 2005). The stratigraphic range of the 'hot shales' in the Central Graben (unit B of the Upper Kimmeridge Clay Formation, Mandal and Farsund Formations) and in the Viking Graben (Draupne Formation) is Volgian–Ryazanian (Vollset & Doré, 1984; Clark *et al.* 1993, Cornford, 1994; Ineson *et al.* 2003; Badics *et al.* 2015; Ziegs *et al.* 2017), comparable to the Bazhenovo Formation in Western Siberia. In some cases the 'hot shale' is overlain by upper Ryazanian black shales, which are less rich in organic carbon (Lott *et al.* 1989). The lithostratigraphy and gamma-ray log patterns of the core sections (Vollset & Doré, 1984; Clark *et al.* 1993; Ineson *et al.* 2003) when using calibrated relationships between gamma-log response and TOC values (Cornford, 1998) suggest an almost uniform distribution of the elevated TOC values within the 'hot shale' units, thus also revealing its resemblance to the Bazhenovo Formation. Kerogen in the 'hot shales' is of Type II, originating from a mixture of degraded terrestrial and planktonic marine OM, resulting in the high hydrogen index values of 350–650 (Cornford, 1994, 1998; Gautier, 2005; Ponsaing *et al.* 2020; see Fig. 4c). The lower interval (upper Kimmeridgian – lower Volgian) of the black shale (TOC, 2–6 wt%) with lower gamma-ray values is present in the Moray Firth, Viking Graben and Norwegian–Danish Basin (Miller, 1990).

In Greenland, the Upper Jurassic – lowermost Cretaceous black shales are well-known but have only been studied in detail in Jameson Land. Here, upper Oxfordian – lower Volgian black shales of the Hareelv Formation, with TOC values of 5–10% and kerogen Type III or Type II–III, seem to be degraded as a result of their pre-oil-window maturity (Bojesen-Koefoed *et al.* 2018; Figs 2, 3b, 4d). Macrofossils recovered from black shale of the Blokelv-1 borehole are represented by ammonites, belemnites, onychites, bivalves and vertebrates, belonging to typical Boreal and Subboreal taxa (Alsen & Piasecki, 2018). Coeval strata of the Kuhn Ø belonging to the upper Oxfordian – lowermost Ryazanian Bernbjerg Formation, are dominated by dark-grey to black mudstones with TOC values of 2.8–5.4% (TOC data for the Volgian part of the succession remain unpublished); these rocks are also rich in ammonites, belemnites and buchiid bivalves (Alsgaard *et al.* 2003; Pauly *et al.* 2013; Kelly *et al.* 2015). The presence of black shale facies was also reported from North Greenland, where black shales of the Ladegardsaen Formation (Kimmeridgian–Volgian) are known

https://doi.org/10.1017/S001675682000076X Published online by Cambridge University Press

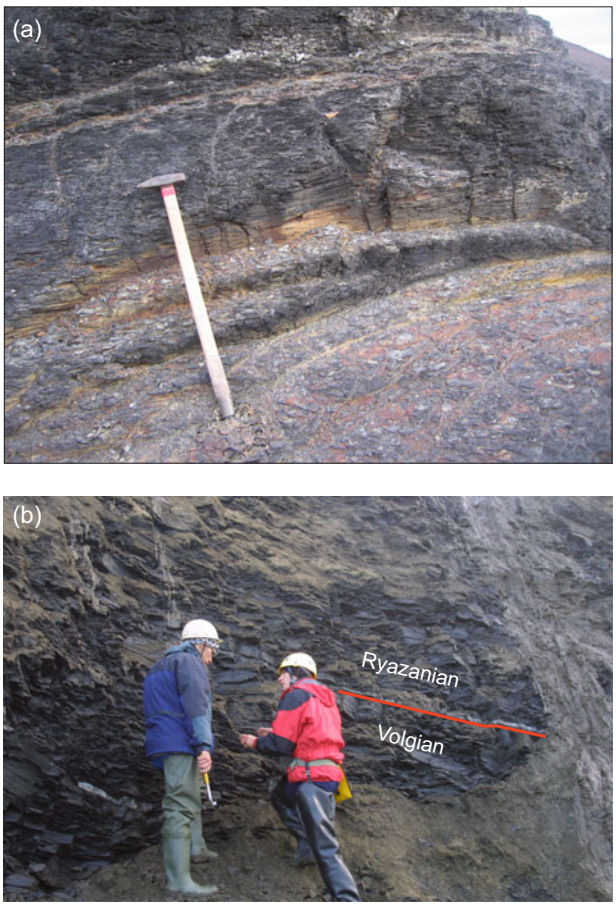

Fig. 8. Black shales of the Boreal type. (a) Kimmeridgian black shales at Myklegardfjellet, Spitsbergen (photograph by DS Zykov). (b) Volgian–Ryazanian boundary beds at Nordvik, northern Siberia (photograph by M Mazuch).

from Peary Land (Håkansson *et al.* 1981), while in Kilen black shales of the Dromledome Formation are Ryazanian – ? Hauterivian in age (Hovikoski *et al.* 2018). No TOC data have been published from north Greenland.

Black shales of the Late Jurassic – earliest Cretaceous age are well-represented in Svalbard (Figs 2, 3c, 8a). In contrast to aforementioned examples, in some cases the oldest black shale occurrences (with TOC contents up to 12%) are of Callovian age (Dypvik, 1985). However, mass deposition of black shales in this area generally began during late Oxfordian time and ended during late Volgian or early Ryazanian time (Koevoets *et al.* 2016, 2019). Two peaks of TOC values are recorded in the black paper shale, traced in both near-shore and offshore areas (Nagy *et al.* 1988; Koevoets *et al.* 2018*a*): upper Oxfordian – lower Kimmeridgian (TOC up to 6–11%); and uppermost middle – upper Volgian (TOC up to *c.* 12–14%) (Fig. 2), with background values oscillating around 1–3%. According to Koevoets *et al.* (2018*a*), the low HI values (50–200) in the black shales result from extensive thermal degradation, as indicated by T_{max} values of 448–476°C (Fig. 4d). These suggest a higher initial quality of kerogen (Type II), which is most likely marine in origin. Black shales belong to the upper part of the Agardhfjellet Formation (Fig. 8a), which is well-exposed in Spitsbergen, and its fossil assemblages have attracted much attention during the last decade (Hammer *et al.* 2013; Delsett *et al.* 2016; Koevoets *et al.* 2016, 2018*a*, *b*, 2019). Ammonites and *Buchia* bivalves are the most typical fossils, but sometimes other bivalves and gastropods as well as belemnites, onychites and echinoderms are also abundant (Hammer *et al.* 2013; Koevoets *et al.* 2018*a*). Vertebrate remains, including skeletons of diverse marine reptiles (Delsett *et al.* 2016) as well as fish bones and scales, are also very typical components of the black shale fossil assemblage (Koevoets *et al.* 2018*b*).

Black shales from the southern part of the Norwegian Sea belong to the Spekk Formation, ranging in age from Oxfordian to Ryazanian (Dalland *et al.* 1988). Sometimes the Spekk Formation is referred to the Volgian–Ryazanian interval only, underlain by the Oxfordian–Kimmeridgian siltstones of the Rogn Formation. The high TOC values (from 4–5% to 10–13%) and mixed Type II and III kerogens were identified for the Spekk Formation of the Haltenbanken area (Cornford, 1998). In the near-shore part of the basin (core 6307/07-U-02) highest TOC values (up to 7%) are reported from the Volgian stage (especially the lower Volgian substage), and show a gradual decline towards the Ryazanian stage (with TOC values up to 4%) (Langrock & Stein, 2004). Black shales in the northern part of the Norwegian Sea shelf (Hekkingen Formation) are of late Oxfordian – Ryazanian age. These rocks are represented by dark silty claystone, which is characterized by the uniformly elevated (2–7%) level of total organic carbon, with a peak in the approximate upper Volgian substage (Smelror *et al.* 2001; Mutterlose *et al.* 2003; Fig. 2). As at other Boreal sites, macrofossils here are dominantly represented by ammonites and *Buchia* bivalves, as revealed from the borehole 6814/04-U-02 (Smelror *et al.* 2001). Very similar patterns of black shale occurrences are reported from the Norwegian sector of the Barents Sea shelf (Langrock *et al.* 2003; Langrock & Stein, 2004; Georgiev *et al.* 2017). Here, these rocks are also of late Oxfordian – late Ryazanian age (Fig. 2). In the southwestern part of the Barents Sea, the maximum TOC (15.4%) and HI (300–430) values and the highest hydrocarbon generation potential (Fig. 4b) have been estimated within the upper Oxfordian – Kimmeridgian Alge Member of the Hekkingen Formation (Helleren, 2019). However, macrofaunas of these black shales are insufficiently known. Only Oxfordian – Kimmeridgian ammonites are well-studied (Wierzbowski *et al.* 2002; Wierzbowski & Smelror, 2020), and very few Ryazanian *Buchia* bivalves and ammonites were mentioned and/or figured from this region (Wierzbowski *et al.* 2011). Information concerning the black shales of the Russian sector of the Barents Sea is very limited, as all boreholes drilled here are poorly sampled, and characteristics of rocks were mainly based on an analysis of geophysical data and cuttings. The range of the black shale facies here can be roughly estimated as Kimmeridgian–Ryazanian. TOC values of these black shales lie mainly between 2 and 23%, but fluctuations of TOC distribution through the succession remains unclear (Basov *et al.* 2009). Fossils recovered from these black shales mainly belong to ammonites and *Buchia*; in addition to these groups, lingulid brachiopods, coleoid hooks and onychites (including big-sized megaonychites) were reported from the Volgian interval of black shales.

Black shales enriched by organic carbon were also reported from the upper Oxfordian – Ryazanian Hofer Formation of Franz-Josef Land (Kosteva, 2005), but information concerning TOC remains unpublished. Leith *et al.* (1992) indicated that Upper Jurassic samples from this area have organic carbon contents of only 1–3%.

Upper Jurassic – Lower Cretaceous black shales are especially well-known in Western Siberia. Although the black shale lithofacies ranges from the upper Oxfordian to the Hauterivian

https://doi.org/10.1017/S001675682000076X Published online by Cambridge University Press

(Braduchan *et al.* 1989), the Volgian–Ryazanian black shales of the famous Bazhenovo Formation (Braduchan *et al.* 1986; Panchenko *et al.* 2015; Ryzhkova *et al.* 2018) and its time equivalents are more widely distributed across Siberia. Upper Oxfordian – Kimmeridgian black shale facies here are restricted by the NE part of Western Siberia. These black shales belong to the Yanov Stan Formation (upper Oxfordian – Ryazanian, up to 300 m), and show relatively low TOC values (2.8% average) with a general trend to gradual TOC rise upsection, with maximum values up to *c.* 8%. As follows from the RockEval data, Type II kerogen and Type III kerogen occurred here in nearly equal quantities (Afanasenkov *et al.* 2018). Several members of the Bazhenovo Formation characterized by different dominant micro- and macrofossil groups can be recognized within the Bazhenovo Formation (Panchenko *et al.* 2015, 2016). In the central regions of Western Siberia (Khanty-Mansiysk–Tyumen), the Bazhenovo Formation as well as its time analogue in the west of this area (lower Tutleim Member) can be subdivided into the lower (lower–middle Volgian) and upper (upper Volgian – Valanginian) members. The lower member (15–20 m) is composed mainly of dark-brown laminated siliceous shales rich in radiolarians, with low (30–40%) clay content and high (5–10%) organic carbon enrichment. Almost pure, devoid of clay, structureless dark chalcedonite with thin radiolarite intercalations prevail near the top (2–5 m) of the lower member. The upper member of Bazhenovo Formation (15–25 m) starts with very dark-brown clayey silicite (2–6 m) abundant in bivalve shells. This thin, but laterally traceable clayey unit corresponds to the upper Volgian substage. It is overlain by thinly laminated black shale with abundant calcareous nannoplankton of Ryazanian age, which is highly enriched in organic carbon (up to 20% and more). Within the upper Valanginian interval, the black shales are gradually followed by terrigenous clays with decreasing TOC, suggesting an increase in sedimentation rates. In the eastern part of Western Siberia (Tomsk region) the lower member, rich in radiolaria, is reduced, and the overlying black shale unit within the upper member, which is highly enriched in organic carbon and calcareous nannoplankton remnants, declines or disappears, while the clayey unit is much thicker. Such a dilution results in lower TOC values (5–7%) on average and a displacement of TOC maxima in the lower member of the Bazhenovo Formation. It is noteworthy that in spite of non-uniformities in the organic carbon distribution in core sections from two different parts of Western Siberia, the numerous RockEval data show mainly Type II kerogen of marine origin (Lopatin & Yemets, 1987; Peters *et al.* 1993; Ulmishek, 1993; Kozlova *et al.* 2015; see Fig. 9c), and the general trend is characterized by a gradual increase in TOC values during Volgian time. This is followed by a gradual decrease during Ryazanian time, although some levels are characterized by extremely high TOC values (Panchenko *et al.* 2016; Fig. 2; Fig. 5d). Highest average values of TOC are reached in the black shales of the central and southwestern regions of Western Siberia (Ponomareva *et al.* 2018). Ammonites (Fig. 6b, e), oysters, *Inoceramus* and *Buchia* bivalves (Fig. 6b, d), fish remains and onychites (Fig. 6a, c) are among the most common fossils of the Bazhenovo Formation (Braduchan *et al.* 1986; Panchenko *et al.* 2015). Surprisingly, large-sized fossil reptiles are extremely rare in this area: only one occurrence of ichthyosaur bones is known to date from the Bazhenovo Formation. This is consistent with the lithofacies characteristics and usually interpreted as resulting from deposition in restricted deep-marine environment persistently prone to anoxic conditions (Zakharov, 2006; Grishkevich, 2018).

Eastwards from Western Siberia, in the Yenissei–Khatanga depression, Upper Jurassic and Lower Cretaceous rocks are mainly represented by shallow-water deposits with low organic carbon contents (cf. Shurygin & Dzyuba, 2015). However, in the north of Central Siberia, from the Khatanga Bay in the west to the Lena River lower reaches in the east, Upper Oxfordian – Ryazanian black shales become the dominant rock type. Only the well-known Nordvik section (Fig. 8b), which is the most thoroughly studied Boreal section across the J/K boundary (Zakharov *et al.* 1983, 2014; Houša *et al.* 2007; Nikitenko *et al.* 2008, 2015; Kashirtsev *et al.* 2018), provides information concerning the organic geochemistry of these black shales. As has been revealed by Zakharov & Yudovny (1974) and recently approved by Kashirtsev *et al.* (2018), typical black shales with elevated TOC values here are mainly restricted to the upper Oxfordian and middle Volgian – Ryazanian substages (Figs 2, 5c). However, their hydrogen index values indicate only kerogen of Type III, with a low contribution of marine OM, probably due to high sedimentation rates and dilution with terrigenous components (Fig. 9d). Fossil assemblages of these black shales are dominated by ammonites, belemnites, onychites and *Buchia* bivalves (Zakharov *et al.* 1983, 2014).

Black shales in Arctic Canada still remain insufficiently studied in terms of high-resolution biostratigraphy and geochemistry. Generally they are restricted to the Kimmeridgian–Ryazanian interval, although locally a first occurrence of black shales could be dated as Oxfordian (Leith *et al.* 1992). Highest TOC values are reported from the Kimmeridgian part of the succession (Gentzis *et al.* 1996), while the Volgian–Ryazanian interval is characterized by less than 5% of TOC. Recent data by Galloway *et al.* (2019) have revealed that the Deer Bay Formation of the Axel Heiberg island is generally characterized by low TOC values throughout the succession. Their two measured sections show median values of TOC 1.6%, with range 0.9–4.6% (Buchanan Lake section) and TOC 1.8%, with range 0.8–5.7% (Geodetic Hills section). Highest TOC values in both sections are recorded near the top of the formation in the upper Valanginian substage. Organic matter is represented either by Type III kerogen (at Buchanan Lake) or by a mixture of Type II and III kerogen (at Geodetic Hills). As well as in other Boreal shaly facies, ammonites and *Buchia* strongly dominate in faunal assemblages of these rocks of Arctic Canada (Jeletzky, 1984).

Rocks that resemble black shales in Northern Alaska belong to the Oxfordian–Valanginian Kingak Shale Formation (Bird & Molenaar, 1987). TOC values reported from these shales are relatively few (mainly less than 2%, see Magoon *et al.* 1987; Bayliss & Magoon, 1988). Imlay (1981) reported ammonites and *Buchia* from Kingak Shale, indicating an early Oxfordian – earliest Ryazanian age of this formation.

3. High-latitude Late Jurassic – earliest Cretaceous black shale occurrences in the Southern Hemisphere

Black shale facies, mainly represented by 'massive' black shale members or formations that resemble black shales of the Boreal type, are common in the high-latitude areas of the Southern Hemisphere (Figs 10, 11). These are the Tithonian – lower Valanginian Vaca Muerta Formation of the Neuquen Basin (Argentina, see Kietzmann *et al.* 2016); upper Callovian – Berriasian Spiti Shale Formation of Nepal (Cariou *et al.* 1994; Enay, 2009); Tithonian black shales of the Suowa Formation, Tibet (Chen *et al.* 2012; Yang *et al.* 2017);

https://doi.org/10.1017/S001675682000076X Published online by Cambridge University Press

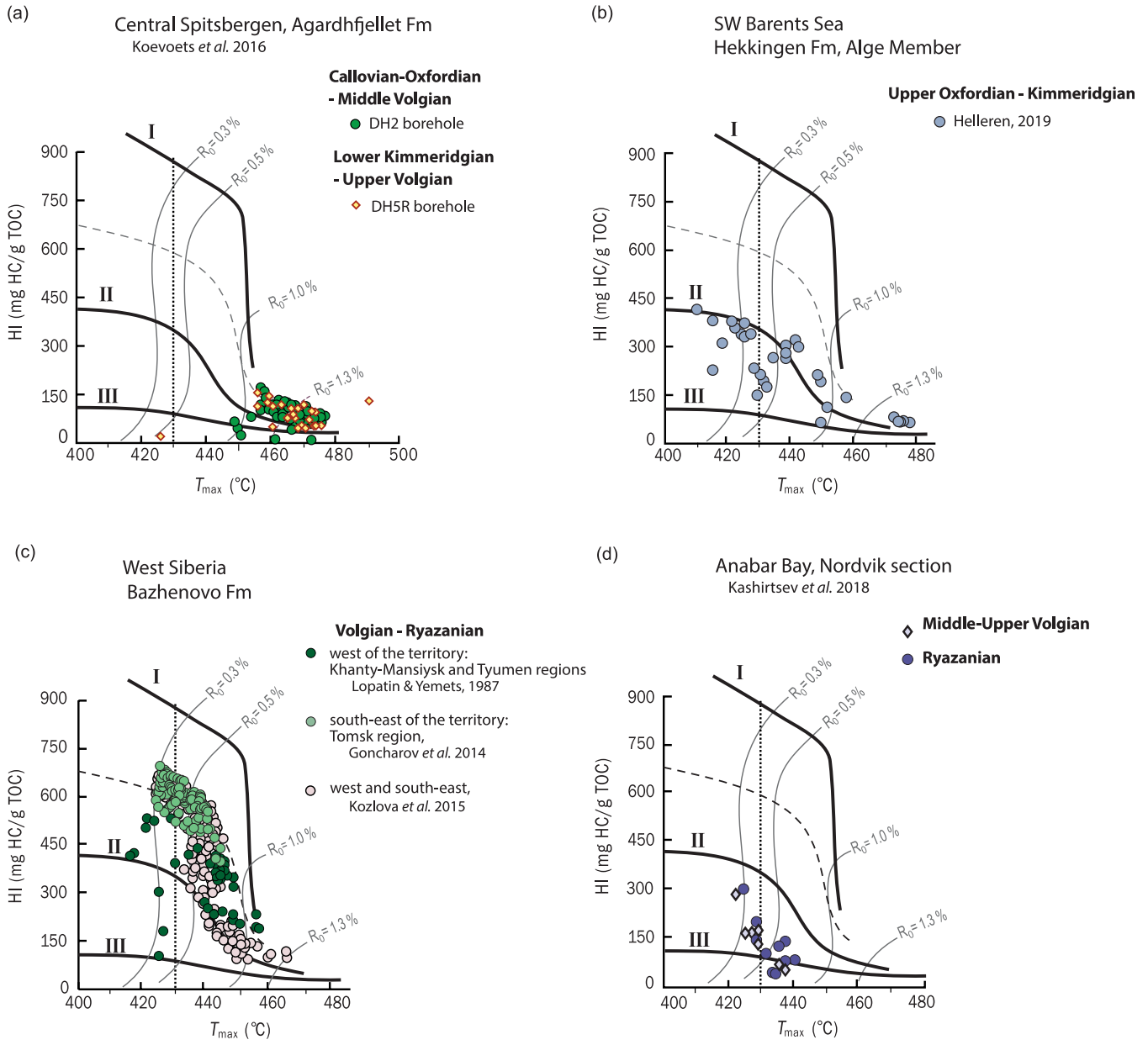

Fig. 9. (a–d) Hydrogen index (HI) versus pyrolysis T_{max} diagram, showing kerogen type and thermal maturity (after Delvaux *et al*. 1990; Tyson, 1995) of Subboreal and Boreal black shales of the Barents Sea region and Siberia. Dashed curve distinguishes kerogen of Type II (marine) and mixed Type II–III (marine and terrestrial). Dotted vertical line (T_{max} = 430° C) subdivides immature and mature kerogen; R_0, vitrinite reflectance.

Kimmeridgian–Tithonian black shales of the Jhuran Formation in Kutch (Arora *et al.* 2015); and Kimmeridgian–Berriasian black shales of the Nordenskjöld Formation, Graham Land, Antarctic (Doyle & Whitham, 1991). Oxfordian–Tithonian black shales of the Falkland Plateau (Deroo *et al.* 1983) are the only Upper Jurassic black shales recorded during the Deep Sea Drilling Program. Macrofossil assemblages of these black shales mainly includes ammonites, vertebrates and, in some cases, *Buchia* homoeomorphs ascribed to *Australobuchia* (Doyle & Whitham, 1991).

All aforementioned high-latitude black shales of the Southern Hemisphere shared many common features with Boreal black shales discussed in the previous section. These are relatively thick black shale units characterized by elevated TOC values. They were deposited in anoxic–dysoxic environments, and characterized by low-diversity benthonic faunas represented by taxa tolerant to low-oxygen contents.

4. Low-latitude Late Jurassic – earliest Cretaceous black shales

The 'Late Jurassic ocean anoxic event' (Nozaki *et al.* 2013; Arora *et al.* 2015) or 'Oxfordian–Kimmeridgian anoxic event' earlier suggested by (Trabucho-Alexandre *et al.* 2012) is not global in the strict sense because low-latitude occurrences of Upper Jurassic – lowermost Cretaceous black shales are scarce and known from only a few areas (Figs 10, 11). These are the upper Oxfordian – Kimmeridgian Haynesville Shale Formation in east Texas and Louisiana (Hammes *et al.* 2011) and the upper Oxfordian – Tithonian black shales of Mexico (La Casita Formation, La Caja

https://doi.org/10.1017/S001675682000076X Published online by Cambridge University Press

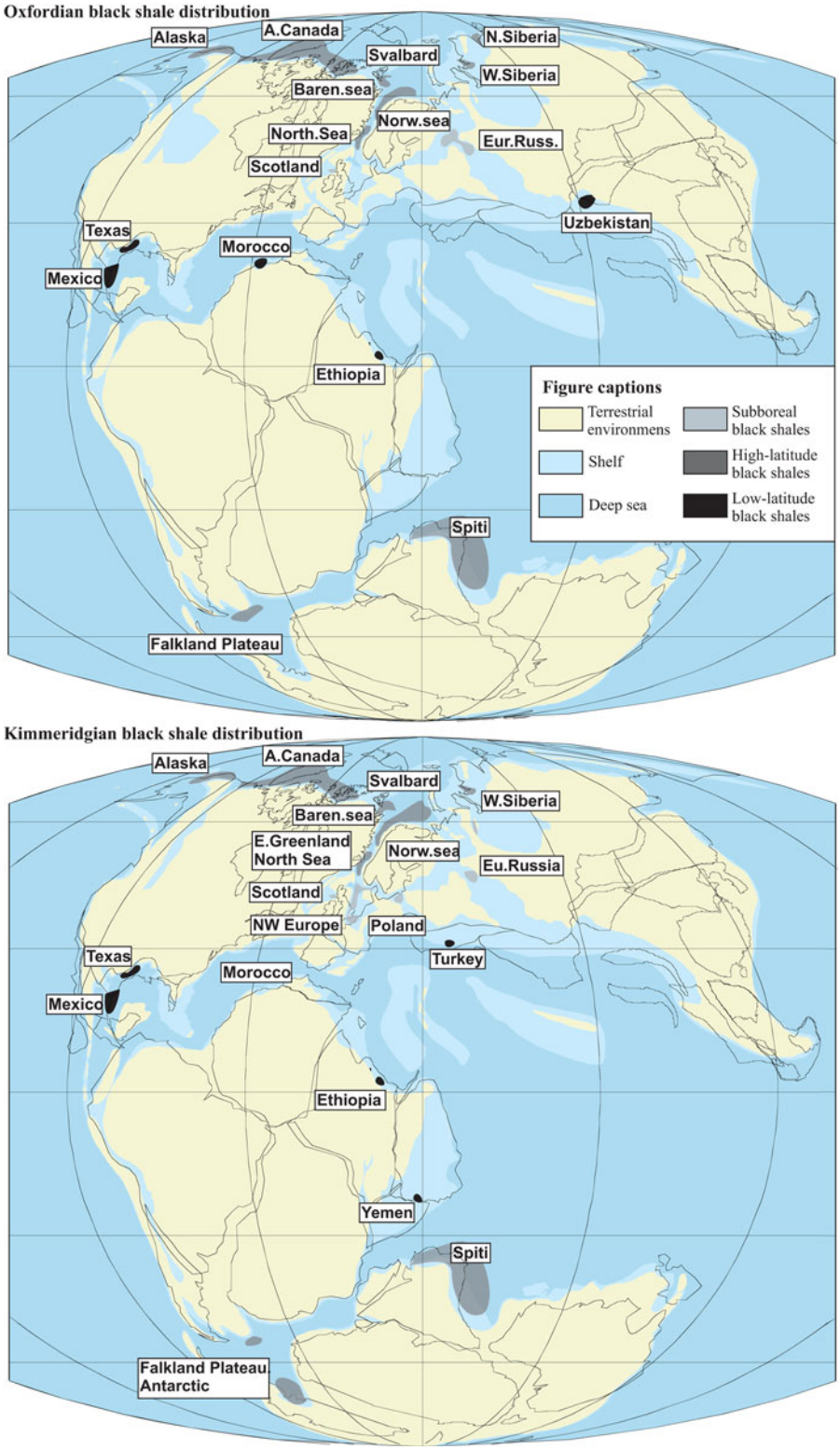

Fig. 10. Oxfordian and Kimmeridgian palaeogeography (after Rees *et al.* 2000, with minor changes) and worldwide distribution of black shales.

Formation, Pimienta Shale Formation; see Goldhammer & Johnson, 2002 for details). Middle Oxfordian black shales showing elevated TOC values (up to 6%) are known in the Khodjaipak Formation, Uzbekistan (Carmeille *et al.* 2020), while Kimmeridgian black marlstones of the Akkuyu Formation (SW Turkey) show very high TOC values (up to 30%, see Baudin *et al.* 1999), comparable with those of Boreal regions. Oxfordian–Kimmeridgian black shales intercalated with limestones were also reported from the Antalo Limestone Formation in Ethiopia (Mohammedyasin *et al.* 2019) and Oxfordian

https://doi.org/10.1017/S001675682000076X Published online by Cambridge University Press

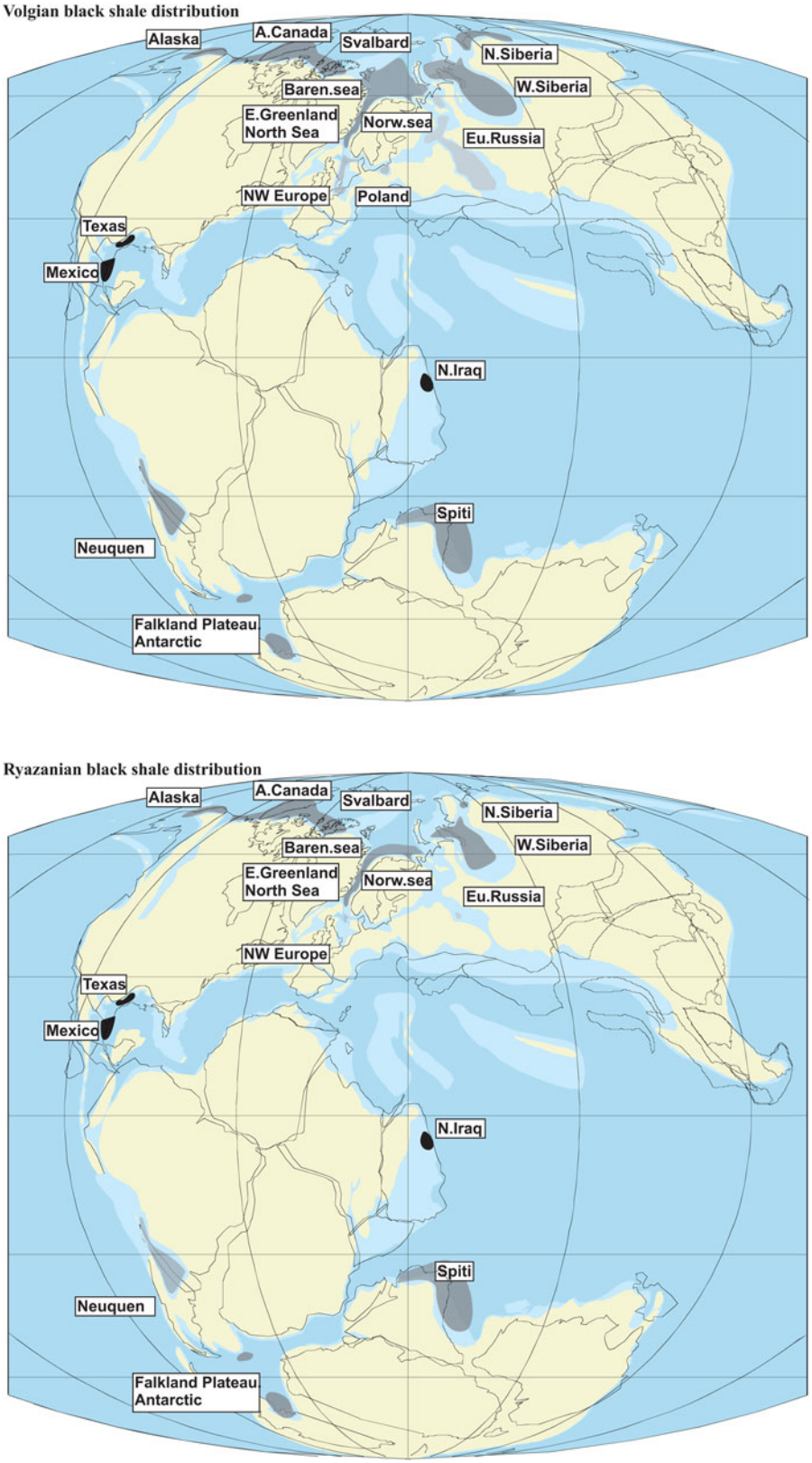

Fig. 11. Volgian and Ryazanian palaeogeography and worldwide black shale distribution.

black shales are known of in Morocco (Davison, 2005). Upper Jurassic black shale occurrences are also known from Yemen (Hakimi & Ahmed, 2016, restricted to Kimmeridgian Madbi Formation) and northern Iraq (Tithonian–Berriasian Chia Gara Formation; see Tobia *et al.* 2019). In all aforementioned examples, low-latitude black shales occur in restricted basins (Figs 10, 11). In contrast to high-latitude black shales, these beds are frequently intercalated with limestones and marls and their deposition seems to be influenced mainly by local environmental factors.

https://doi.org/10.1017/S001675682000076X Published online by Cambridge University Press

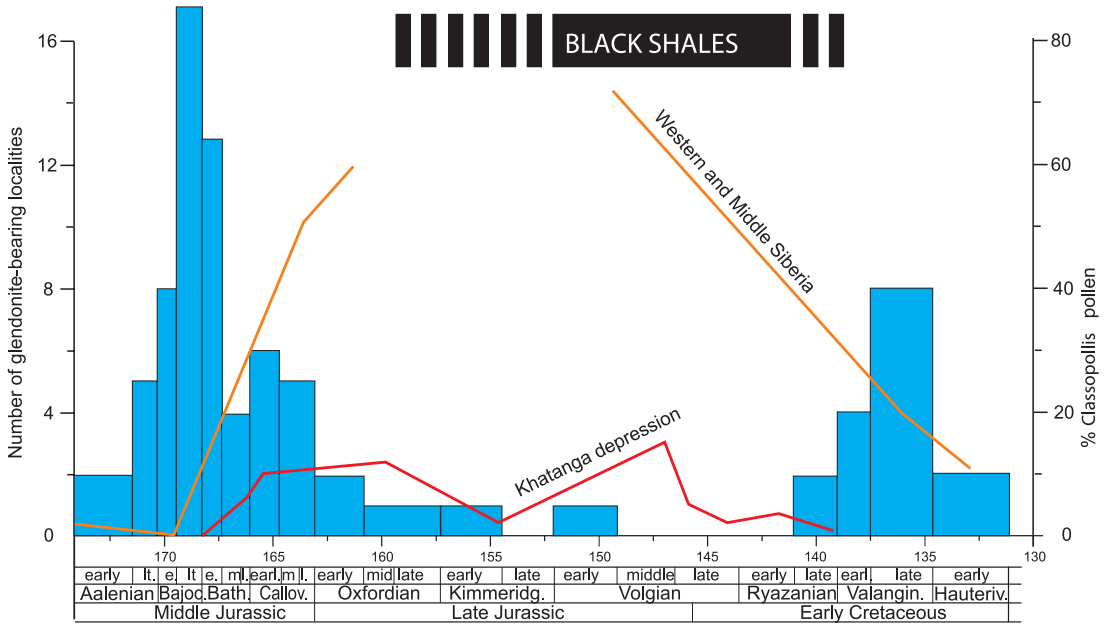

Fig. 12. Climate indicators and black shale distribution in Western and north of Eastern Siberia. Blue bars showing amount of glendonite-bearing sites (Rogov *et al.* 2019, with minor changes), while orange and red lines showing *Classopollis* pollen abundance (based on Vakhrameyev, 1982, with some additions from Ilyina, 1985; Nikitenko *et al.* 2015).

5. Key features of the Late Jurassic – earliest Cretaceous high-latitude shelf dysoxic–anoxic event

As emphasized in Section 1, in contrast to OAEs, the onset and offset of the SDAE are strongly diachronous in different basins and sub-basins. In all cases, however, the duration of black shale deposition was very long compared with those of OAE-related black shales, indicating nearly constant presence of anoxic–dysoxic near-bottom depositional conditions over periods of 10–20 Ma. The very widespread geographic distribution of these black shale facies in high latitudes excludes any significant influence of local factors on their deposition, while the traceability of individual black shale beds and their relationship with overlying and underlying units were controlled by local environmental conditions. Although different regions are characterized by different patterns of TOC values through time, at least for black shales of the Boreal type, maximum TOC contents were reported for the upper Volgian, that is, for the Jurassic–Cretaceous transitional strata. Although some attempts at chemostratigraphic correlation of these rocks were undertaken recently (Turner *et al.* 2019), deposition of high-latitude Upper Jurassic – lowermost Cretaceous black shales are not associated with any significant carbon isotope excursions. The only carbon isotope excursion during middle Volgian time, the so-called VOICE (Volgian Isotopic Carbon Excursion), can be recognized in some Boreal areas (Hammer *et al.* 2012; Koevoets *et al.* 2016; Galloway *et al.* 2019); in contrast to excursions related to the typical OAEs it is relatively long, spanning nearly the whole middle Volgian age, and showing some diachroneity between the basins. The onset of black shale deposition was strongly asynchronous in the different basins and even different sub-basins, and the same is also true for the termination of black shale deposition with the end of the SDAE.

By comparison with coeval units deposited in the well-oxygenated environments, these black shales are characterized by a very low diversity of benthic organisms represented by a few dominant genera tolerant of low oxygen contents, especially by burrowing suspension-feeding bivalves (Oschmann, 1988, 1994) as well as by nektonic and planktonic animals. In black shales of the Boreal type, benthic fossils usually only occur in thin intervals, which indicate short-time increases in oxygen contents near the sea floor, while other parts of the successions are typically barren of benthic macrofossils. Nevertheless, these long-lasting anoxic conditions did not cause significant faunal turnover or extinction.

6. Possible causes of the Late Jurassic – earliest Cretaceous shelf dysoxic–anoxic events

Rising temperatures accompanied by increased productivity, together with slow ocean circulation, are considered among the factors responsible for prolonged black shale deposition in the Arctic (Georgiev *et al.* 2017). Indeed, gradual warming during the Late Jurassic epoch in the Boreal areas is supported by palynology (Dzyuba *et al.* 2018), clay mineralogy (Ruffell *et al.* 2002) and oxygen stable isotope data (Price & Rogov, 2009; Zakharov *et al.* 2014; Dzyuba *et al.* 2018). Cold-water glendonite pseudomorphs are common in the Middle Jurassic deposits of Siberia (Morales *et al.* 2017), but they rarely occur in the Upper Jurassic deposits. Glendonites are absent from the upper Kimmeridgian – lower Ryazanian interval of Siberia (Fig. 12). However, additional factors can be invoked to explain such unique SDAE, because other Mesozoic warming events are not associated with such long-time black shale deposition. It is very possible that, in tandem with warming and changes in oceanic circulation caused by Pangaea break-up, significant changes in the plankton ecosystems could be responsible for long-lasting high productivity. Relatively higher humidity in the Subboreal and Boreal realms compared with low-latitude territories caused more precipitation and more intensive land drainage; the chemical weathering therefore prevailed, at least periodically (or seasonally). Hypopycnal plumes of muddy freshwater could have supplied high amounts of dissolved nutrients to the basins. This led to unfavourable conditions for accustomed

https://doi.org/10.1017/S001675682000076X Published online by Cambridge University Press

marine plankton in the surface waters because of their opacity, abnormal salinity or 'nutrient oversaturation'; their high buoyancy prevented mixing and contributed to stratification. Such conditions in the upper photic zone could cause rapid growth of new, more tolerant, planktonic communities. Periodical (or seasonal) restoration of such conditions was important for long-lasting changes of planktonic communities, resulting in black shale deposition directly or indirectly. In our opinion, immigration of calcareous nannoplankton to high latitudes is an indicator of such a new but very widespread ecological condition in the Subboreal and Boreal seas.

Enhanced productivity of high-latitude basins may have had a significant influence on black shale deposition. Some intervals of the Bazhenovo Formation are so enriched by radiolarians (Khotylev *et al.* 2019) that they are considered here as rock-building, while other intervals consist mainly of calcareous nannoplankton (Zanin *et al.* 2012). However, silicites, typical of the Bazhenovo Formation, rarely occur outside of Western Siberia.

In our opinion, immigration of calcareous nannoplankton to high latitudes is especially important for long-lasting changes of plankton communities and the resulting black shale deposition. It should be noted that coccolithophores, which originated during the Triassic Period (Mutterlose *et al.* 2005), are now responsible for much of the primary oceanic productivity (Malone, 1971; Rost & Riebesell, 2004). During the Late Jurassic epoch, calcareous nannoplankton shows a significant growth in diversity (Bown *et al.* 2004; Suchéras-Marx *et al.* 2019), but in high-latitude Arctic it is only recognized near the Jurassic–Cretaceous transition (Smelror *et al.* 1998; Mutterlose *et al.* 2003; Zanin *et al.* 2012; *Pauly et al.* 2013; Rogov & Ustinova, 2018). Calcareous nannoplankton taxa have therefore controlled an increase in primary productivity, and an ecosystem disturbance seems to be one of the causes of Late Jurassic – earliest Cretaceous high-latitude SDAE. This hypothesis should be investigated in future studies. It should be noted that the onset of the studied interval of black-shale deposition across the Jurassic–Cretaceous boundary coincides with a shift from abiotic to biotic control on evolution of calcareous plankton (Eichenseer *et al.* 2019). Among the other biotic factors, radiolarian blooms should also be considered as regionally responsible for black-shale deposition, that is, for the Bazhenov Formation of the Western Siberia (Khotylev *et al.* 2019). Moreover, mass occurrences of radiolarians were also considered as very important for deposition of the Late Devonian black shales in European Russia (Afanasieva & Mikhailova, 2001) However, among the studied Upper Jurassic – lowermost Cretaceous successions with black shale abundance, there are very few showing mass occurrence of radiolarians. In these cases, radiolarians are easily visible in thin-sections, and these microfossils became rock-forming.

Reduced salinity can also be favourable for black shale deposition. For example, recent studies of the Toarcian strata of the Cleveland Basin have revealed a significant salinity drop during the black shale interval associated with the Toarcian OAE, in spite of the common occurrence of ammonites that sharing a low tolerance to salinity decrease with other cephalopods (Remírez & Algeo, 2020). However, the gradual decrease of salinity in the Middle Russian Sea during Oxfordian–Kimmeridgian time, recognized through clumped isotope studies (Wierzbowski *et al.* 2018), shows no correlation with the prominent black shale horizons that occurred mainly in two very short intervals (at the beginning of the late Oxfordian and middle part of the late Kimmeridgian Mutabilis Chron). Although reduced salinity of the Arctic area was suggested as the one of the factors controlling regional distribution of faunas by Hallam (1969), any evidence of a long-term drop in salinity in high-latitude areas during Late Jurassic – earliest Cretaceous time is missing. During the period considered here, both planktonic and nektonic faunas in high latitudes were nearly of the same type as before or after the SDAE, and were represented by the same taxa (at least at the family level).

7. Conclusions

The Late Jurassic – earliest Cretaceous episode of prolonged (10–20 Ma) black shale deposition in extra-tropical latitude areas is identified as a shelf dysoxic–anoxic event (SDAE). This specific type of anoxic event differs from typical OAEs. During the Late Jurassic – earliest Cretaceous time interval, OM-rich sediment accumulated mainly in the high latitudes. The onset and termination of SDAE was diachronous in separate palaeobasins. Subboreal and Boreal patterns of black shale deposition, caused by variations in the stability of oxygen-depleted environments, has been recognized. Among the main drivers of the SDAE, global climatic warming led to significant palaeo-oceanographic changes favouring a sluggish stratification-prone circulation pattern, driving the advancement of widespread dysoxia–anoxia-prone environments onto shallow shelves. These could have led to a disturbance in planktonic ecosystems and to an invasion of calcareous, siliceous and organic-walled nannoplankton to high-latitude palaeobasins, providing huge reserves for warmer and more transparent water masses during the considered period.

Acknowledgements. This study was supported by RSF grant 17-17-01171. The authors thank IV Panchenko (JSC MiMGO, Moscow) and YuA Gatovsky (Moscow State University, Moscow) for providing fossil specimens from western Siberia figured in this article. Two anonymous reviewers are kindly acknowledged for their valuable comments. We are especially grateful to Bas van de Schootbrugge for his work on improvement of the English language.

References

Afanasenkov AP, Petrov AL and Grayzer EM (2018) Geochemical description and oil-and-gas generation potential of Mesozoic formations within the Gydan and Yenisei-Khatanga oil and gas bearing regions. *Oil and Gas Geology* **6**, 109–27 (in Russian). doi: 10.31087/0016-7894-2018-6-109-127

Afanasieva MS and Mikhailova MV (2001) The Domanik Formation of the Timan-Pechora basin: Radiolarians, biostratigraphy, and sedimentation conditions. *Stratigraphy and Geological Correlation* **9**, 419–40.

Alsen P and Piasecki S (2018) Biostratigraphy of the Hareelv Formation (Upper Jurassic) in the Blokelv-1 core, Jameson Land, central East Greenland. *Geological Survey of Denmark and Greenland Bulletin* **42**, 15–37. doi: 10.34194/geusb.v42.4308

Alsgaard PC, Felt VL, Vosgerau H and Surlyk F (2003) The Jurassic of Kuhn Ø, North-East Greenland. *Geological Survey of Denmark and Greenland Bulletin* **1**, 865–92.

Arora A, Banerjee S and Dutta S (2015) Black shale in late Jurassic Jhuran Formation of Kutch: possible indicator of oceanic anoxic event? *Journal of the Geological Society of India* **85**, 265–78. doi: 10.1007/s12594-015-0215-6

Arthur MA and Sageman BB (1994) Marine black shales: depositional mechanisms and environments of ancient deposits. *Annual Review in Earth and Planetary Sciences* **22**, 499–551. doi: 10.1146/annurev.ea.22.050194.002435

Badics B, Avu A and Mackie S (2015) Assessing source rock distribution in Heather and Draupne Formations of the Norwegian North Sea: a workflow using organic geochemical, petrophysical, and seismic character. *Interpretation* **3**, SV45–68. doi: 10.1190/INT-2014-0242.1

https://doi.org/10.1017/S001675682000076X Published online by Cambridge University Press

Baraboshkin EYu (2004) Boreal-Tethyan correlation of Lower Cretaceous ammonite scales *Moscow University Geology Bulletin* **59**, 9–20.

Basov VA, Nikitenko BL and Kupriyanova NV (2009) Lower–Middle Jurassic foraminiferal and ostracode biostratigraphy of the Barents Sea shelf. *Russian Geology and Geophysics* **50**, 396–416. doi: 10.1016/j.rgg.2008.08.006

Baudin F, Tribovillard N, Laggoun-Défarge F, Lichtfouse E, Monod O and Gardin S (1999) Depositional environment of a Kimmeridgian carbonate 'black band'(Akkuyu Formation, south-western Turkey). *Sedimentology* **46**, 589–602. doi: 10.1046/j.1365-3091.1999.00226.x

Bayliss G and Magoon LB (1988) Organic facies and thermal maturity of sedimentary rocks in the National Petroleum Reserve in Alaska. *United States Geological Survey Professional Paper* **1399**, 489–518.

Bird KJ and Molenaar CM (1987) Stratigraphy. In *Petroleum Geology of the Arctic National Wildlife Refuge* (eds KJ Bird and LB Magoon), pp. 37–59. Northeastern Alaska: United States Geological Survey, Bulletin 1778.

Bojesen-Koefoed JA, Bjerager M, Nytoft HP, Petersen HI, Piasecki S and Pilgaard A (2018) Petroleum potential of the Upper Jurassic Hareelv Formation, Jameson Land, East Greenland. *Geological Survey of Denmark and Greenland Bulletin* **42**, 85–113. doi: 10.34194/geusb.v42.4314

Bown PR, Lees JA and Young JR (2004) Calcareous nannoplankton evolution and diversity through time. In *Coccolithophores. From Molecular Processes to Global Impact* (eds HR Thierstein and JR Young), pp. 481–508. Berlin, Heidelberg: Springer.

Braduchan YuV, Gurari FG, Zakharov VA, Bulynnikova SP, Vyachkileva NP, Golbert AV, Klimova IG, Kozlova GE, Lebedev AI, Mesezhnikov MS, Nalnyaeva TI and Turbina AS (1986) Bazhenovo horizon of West Siberia (stratigraphy, paleogeography, ecosystem, oil-and-gas content). *Siberian Branch of the Russian Academy of Science, Transactions of the Institute of Geology and Geophysics*, **649**, 1–216 (in Russian).

Braduchan YuV, Zakharov VA and Mesezhnikov MS (1989) Stratigraphy and depositional conditions of bituminous deposits of Upper Jurassic - Neocomian of the European part of USSR and Western Siberia. In *Sedimentary Cover of the Earth in Space and Time. Stratigraphy and Paleontology* (ed. BS Sokolov), pp. 108–15. Moscow: Nauka (in Russian).

Bragin VYu, Dzyuba OS, Kazansky AYu and Shurygin BN (2013) New data on the magnetostratigraphy of the Jurassic–Cretaceous boundary interval, Nordvik Peninsula (northern East Siberia). *Russian Geology and Geophysics* **54**, 335–48. doi: 10.1016/j.rgg.2013.02.008

Bushnev DA, Shchepetova EV and Lyyurov SV (2006) Organic geochemistry of Oxfordian carbon-rich sedimentary rocks of the Russian Plate. *Lithology and Mineral Resources* **41**, 423–34. doi: 10.1134/s0024490206050038

Callomon JH and Cope JCW (1971) The stratigraphy and ammonite succession of the Oxford and Kimmeridge clays in the Warlingham Borehole. *Bulletin of the Geological Survey of Great Britain* **36**, 147–76.

Cariou E, Enay R, Bassoullet J-P and Colchen M (1994) Biochronologie du Jurassique moyen de la Thakkhola (Népal central) et biogéographie du domaine himalayen. *Comptes Rendus de l'Académie des Sciences, Paris, Séries II* **318**, 93–9.

Carmeille M, Bourillot R, Pellenard P, Dupias V, Schnyder J, Riquier L, Mathieu O, Brunet MF, Enay R, Grossi V and Gaborieau C (2020) Formation of microbial organic carbonates during the late Jurassic from the Northern Tethys (Amu Darya Basin, Uzbekistan): implications for Jurassic anoxic events. *Global and Planetary Change* **186**, 103127. doi: 10.1016/j.gloplacha.2020.103127

Cecca F (1999) Palaeobiogeography of Tethyan ammonites during the Tithonian (latest Jurassic). *Palaeogeography, Palaeoclimatology, Palaeoecology* **147**, 1–37. doi: 10.1016/s0031-0182(98)00149-7

Chen L, Tien-Shun Lin A, Da X, Yi H, Tsai LL-Y and Xu G (2012) Sea-level changes recorded by Cerium anomalies in the Late Jurassic (Tithonian) black rock series of Qiangtang Basin, North-Central Tibet. *Oil Shale* **29**, 18–35. doi: 10.3176/oil.2012.1.03

Clark DN, Riley LA and Ainsworth NR (1993) Stratigraphic, structural and depositional history of the Jurassic in the Fisher Bank Basin, UK North Sea. *Petroleum Geology of Northwest Europe: Proceedings of the 4th Conference* (ed. by JR Parker), pp. 415–24. Geological Society of London.

Cope JCW (1967) The palaeontology and stratigraphy of the lower part of the Upper Kimmeridge Clay of Dorset. *Bulletin of the British Museum (Natural History) Geology* **15**, 1–79.

Cope JCW (1978) The ammonite fauna and stratigraphy of the upper part of the Upper Kimmeridge Clay of Dorset. *Palaeontology* **21**, 469–533.

Cornford C (1994) Mandal-Ekofisk petroleum system in the Central Graben of the North Sea. In *The Petroleum System from Source to Trap* (eds LB Magoon and WG Dow), pp. 523–39. American Association of Petroleum Geologists, Memoir no. **60**. doi: 10.1306/m60585c33

Cornford C (1998) Source rocks and hydrocarbons of the North Sea. In *Petroleum Geology of the North Sea*, 4th ed. (ed. KW Glennie), pp. 376–462. London: Blackwell Science Ltd.

Dalland A, Worsley D and Ofstad K (1988) A lithostratigraphic scheme for the Mesozoic and Cenozoic succession off shore mid- and northern Norway. *Norwegian Petroleum Directorate Bulletin* **4**, 1–65.

Davison I (2005) Central Atlantic margin basins of North West Africa: geology and hydrocarbon potential (Morocco to Guinea). *Journal of African Earth Sciences* **43**, 254–74. doi: 10.1016/j.jafrearsci.2005.07.018

Delsett LL, Novis LK, Roberts AJ, Koevoets MJ, Hammer Ø, Druckenmiller PS and Hurum JH (2016) The Slottsmoya marine reptile Lagerstatte: depositional environments, taphonomy and diagenesis. In *Dinosaurs and Other Extinct Saurians: A Historical Perspective* (eds RTJ Moody, E Buffetaut, D Naish and DM Martill), pp. 165–88. Geological Society of London, Special Publication no. **434**. doi: 10.1144/SP434.2

Delvaux D, Martin H, Leplat P and Paulet J (1990) Geochemical characterization of sedimentary organic matter by means of pyrolysis kinetic parameters. *Organic Geochemistry* **16**, 175–87. doi: 10.1016/0146-6380(90)90038-2

Deroo G, Herbin JP and Roucaché J (1983) Organic geochemistry of Upper Jurassic–Cretaceous sediments from Site 511, Leg 71, Western South Atlantic. *Initial Reports of the Deep Sea Drilling Project* **71**, 1001–13. doi: 10.2973/dsdp.proc.71.137.1983

Doyle P and Whitham AG (1991) Palaeoenvironments of the Nordenskjöld Formation: an Antarctic Late Jurassic-Early Cretaceous black shale-tuff sequence. In *Modern and Ancient Continental Shelf Anoxia* (eds RV Tyson and TH PEarson), pp. 397–414. Geological Society of London, Special Publication no. 58. doi: 10.1144/gsl.sp.1991.058.01.25

Dypvik H (1985) Jurassic and Cretaceous black shales of the Janusfjellet Formation, Svalbard, Norway. *Sedimentary Geology* **41**, 235–48. doi: 10.1016/0037-0738(84)90064-2

Dzyuba OS, Pestchevitskaya EB, Urman OS, Shurygin BN, Alifirov AS, Igolnikov AE and Kosenko IN (2018) The Maurynya section, West Siberia: a key section of the Jurassic-Cretaceous boundary deposits of shallow marine genesis. *Russian Geology and Geophysics* **59**, 864–90. doi: 10.1016/j.rgg.2018.07.010

Eichenseer K, Balthasar U, Smart CW, Stander J, Haaga KA and Kiessling W (2019) Jurassic shift from abiotic to biotic control on marine ecological success. *Nature Geoscience* **12**, 638–42. doi: 10.1038/s41561-019-0392-9

Enay R (1972) Paléobiogéographie des ammonites du Jurassique terminal (Tithonique/Volgien/Portlandien sl) et mobilité continentale. *Geobios* **5**, 355–407. doi: 10.1016/s0016-6995(72)80013-5

Enay R (2009) Les faunes d'ammonites de l'Oxfordien au Tithonien et la biostratigraphie des Spiti-shales (Callovien supérieur-Tithonien) de Thakkhola, Népal central. *Documents des Laboratoires de Géologie, Lyon* **166**, 1–350.

Etches S and Clarke J (1999) *Steve Etches Kimmeridge Collection Illustrated Catalogue*. Privately printed, Chandler's Ford, Hants (with additional pages added in 2000 and 2001), 131 pp.

Gallois RW (2004) The Kimmeridge Clay: the most intensively studied formation in Britain. *Open University Geological Society Journal* **25**, 33–38.

Gallois RW (2005) Correlation of the Kimmeridgian succession of the Normandy coast, northern France with that of the Dorset-type area, southern England. *Comptes rendus Geosciences* **337**, 347–55. doi: 10.1016/j.crte.2004.12.001

Gallois RW (2011) A revised description of the lithostratigraphy of the Kimmeridgian-Tithonian and Kimmeridgian-Volgian boundary beds at Kimmeridge, Dorset, UK. *Geoscience in South-West England* **12**, 288–94.

Galloway J, Vickers M, Price G, Poulton T, Grasby S, Hadlari T, Beauchamp B and Sulphur K (2019) Finding the VOICE: organic carbon isotope chemostratigraphy of the Late Jurassic-Early Cretaceous of Arctic Canada. *Geological Magazine*, published online 20 December 2019, 1–15. doi: 10.1017/s0016756819001316

Gautier DL (2005) Kimmeridgian Shales Total Petroleum System of the North Sea Graben Province. *U.S. Geological Survey Bulletin* **2204-C**, 1–24. doi: 10.3133/b2204c

Gavrilov YuO, Shchepetova EV and Shcherbinina EA (2014) Sedimentological and geochemical conditions of carbonaceous units occurrences in Mesozoic palaeobasins of the European part of Russia. *Geresources, Geoenergetics, Geopolitics* **1**, 1–30 (in Russian).

Gentzis T, Goodarzi F and Embry AF (1996) Thermal maturation, potential source rocks and hydrocarbon generation in Mesozoic rocks, Lougheed Island area, Central Canadian Arctic archipelago. *Marine and Petroleum Geology* **13**, 879–905. doi: 10.1016/s0264-8172(96)00028-1

Georgiev SV, Stein HJ, Hannah JL, Xu G, Bingen B and Weiss HM (2017) Timing, duration, and causes for Late Jurassic–Early Cretaceous anoxia in the Barents Sea. *Earth and Planetary Science Letters* **461**, 151–62. doi: 10.1016/j.epsl.2016.12.035

Geyssant JR, Vidier J-P, Herbin J-P, Proust J-N and Deconinck J-F (1993) Biostratigraphie et paléoenvironnement des couches de passage Kimméridgien/Tithonien du Boulonnais (Pas-de-Calais): nouvelles données paléontologiques (ammonites), organisation séquentielle et contenu en matière organique. *Géologie de la France* **4**, 11–24.

Głowniak E, Kiselev DN, Rogov M, Wierzbowski A and Wright J (2010) The Middle Oxfordian to lowermost Kimmeridgian ammonite succession at Mikhalenino (Kostroma District) of Russian Platform, and its stratigraphical and palaeogeographical importance. *Volumina Jurassica* **VIII**, 8–45.

Goldhammer RK and Johnson CA (2002) Middle Jurassic-Upper Cretaceous paleogeographic evolution and sequence-stratigraphic framework of the northwest Gulf of Mexico rim. In *The Western Gulf of Mexico Basin: Tectonics, Sedimentary Basins, and Petroleum Systems* (eds C Bartolini, RT Buffler, and A Cantú-Chapa), 45–81. American Association of Petroleum Geologists, Memoir no. 75. doi: 10.1306/m75768c3

Goncharov IV, Fadeeva SV, Samoilenko VV, Oblasov NV and Bakhtina ES (2014) Generation potential of organic matter Bazhenov Formation rocks in the south-east of Western Siberia (Tomsk region). *Neftyanoe khozyaystvo = Oil Industry* **12**, 12–16 (in Russian).

Grishkevich VF (2018) Neocomian paleogeography, gas hydrate cementation of sediments, and abnormal sequences of the Bazhenov Formation (West Siberia). *Russian Geology and Geophysics* **59**, 157–67. doi: 10.1016/j.rgg.2018.01.013

Håkansson E, Birkelund T, Piasecki S and Zakharov V (1981) Jurassic–Cretaceous boundary strata of the extreme Arctic (Peare Land, North Greenland). *Bulletin of the Geological Society of Denmark* **30**, 11–42.

Hakimi MH and Ahmed AF (2016) Petroleum generation modeling of the organic-rich shales of Late Jurassic–Early Cretaceous succession from Mintaq-01 well in the Wadi Hajar sub-basin, Yemen. *Canadian Journal of Earth Sciences* **53**, 1053–72. doi: 10.1139/cjes-2015-0224

Hallam A (1969) Faunas realms and facies in the Jurassic. *Palaeontology* **12**, 1–18.

Hammer Ø, Collignon M and Nakrem HA (2012) Organic carbon isotope chemostratigraphy and cyclostratigraphy in the Volgian of Svalbard. *Norwegian Journal of Geology* **92**, 103–12.

Hammer Ø, Hryniewicz K, Hurum JH, Høyberget M, Knutsen EM and Nakrem HA (2013) Large onychites (cephalopod hooks) from the Upper Jurassic of the Boreal Realm. *Acta Palaeontologica Polonica* **58**, 827–35. doi: 10.4202/app.2012.0020

Hammes U, Hamlin HS and Ewing TE (2011) Geologic analysis of the Upper Jurassic Haynesville Shale in east Texas and west Louisiana. *American Association of Petroleum Geologists Bulletin* **95**, 1643–66. doi: 10.1306/02141110128

Hantzpergue P, Baudin F, Mitta V, Olferiev A and Zakharov V (1998) The Upper Jurassic of the Volga basin: ammonite biostratigraphy and occurrence of organic-carbon rich facies. Correlations between boreal-subboreal and submediterranean provinces. *Mémoires du Muséum national d'histoire naturelle* **179**, 9–33.

Hatem E, Tribovillard N, Averbuch O, Bout-Roumazeilles V, Trentesaux A, Deconinck J-F, Baudin F and Adatte T (2018) Small-scaled lateral variations of an organic-rich formation in a ramp-type depositional environment (the Late Jurassic of the Boulonnais, France): impact of the clastic supply. *Bulletin de la Société Géologique de France*, **188**, 1–17. doi: 10.1051/bsgf/2017193

Helleren S (2019) Lateral compositional variations in the Upper Jurassic source rock in the southwestern Barents Sea – an organic or inorganic disclosure. M.Sc. thesis, University of Stavanger, Norway. Published thesis.

Herbin JP, Fernandez-Martinez JL, Geyssant JR, Albani AEl, Deconinck JF, Proust JN, Colbeaux JP and Vidier JP (1995) Sequence stratigraphy of source rocks applied to the study of the Kimmeridgian/Tithonian in the north-west European shelf (Dorset/UK, Yorkshire/UK and Boulonnais/France). *Marine and Petroleum Geology* **12**, 177–94. doi: 10.1016/0264-8172(95)92838-n

Houša V, Pruner P, Zakharov VA, Kostak M, Chadima M, Rogov MA, Šlechta S and Mazuch M (2007) Boreal–Tethyan correlation of the Jurassic–Cretaceous boundary interval by magneto- and biostratigraphy. *Stratigraphy and Geological Correlation* **15**, 297–309. doi: 10.1134/s0869593807030057

Hovikoski J, Pedersen GK, Alsen P, Lauridsen BW, Svennevig K, Nøhr-Hansen H, Sheldon E, Dybkjær K, Bojesen-Koefoed J, Piasecki S, Bjerager M and Ineson J (2018) The Jurassic–Cretaceous lithostratigraphy of Kilen, Kronprins Christian Land, eastern North Greenland. *Bulletin of the Geological Society of Denmark* **66**, 61–112.

Ilyasov VS, Staroverov VN and Vorobyeva EV (2018) Geochemical characteristics of organic matter in the Upper Jurassic organic-rich shales. *Volga and Pricaspian Region Resources* **93**, 26–36 (in Russian).

Ilyina VI (1985) Jurassic Palynology of Siberia. Moscow: Nauka. *Siberian Branch of the Russian Academy of Sciences, Transactions of the Institute of Geology and Geophysics* **638**, 1–237 (in Russian).

Imlay RW (1981) Late Jurassic ammonites from Alaska. *United States Geological Survey Professional Paper* **1190**, 1–40. doi: doi.org/10.3133/pp1190

Ineson JR, Bojesen-Koefoed JA, Dybkjær K and Nielsen LH (2003) Volgian–Ryazanian 'hot shales' of the Bo Member (Farsund Formation) in the Danish Central Graben, North Sea: stratigraphy, facies and geochemistry *Geological Survey of Denmark and Greenland Bulletin* **1**, 403–36.

Jeletzky JA (1984) Jurassic-Cretaceous Boundary Beds of western and Arctic Canada and the problem of the Tithonian-Berriasian stages in the Boreal Realms. *Geological Association of Canada Special Paper* **27**, 175–255.

Jenkyns HC (1999) Mesozoic anoxic events and palaeoclimate. *Zentralblatt für Geologie und Paläontologie* **1997**, 943–9.

Jenkyns HC (2010) Geochemistry of oceanic anoxic events. *Geochemistry, Geophysics, Geosystems* **11**, Q03004, doi: 10.1029/2009GC002788

Kashirtsev VA, Nikitenko BL, Peshchevitskaya EB and Fursenko EA (2018) Biogeochemistry and microfossils of the Upper Jurassic and Lower Cretaceous, Anabar Bay, Laptev Sea. *Russian Geology and Geophysics* **59**, 386–404. doi: 10.1016/j.rgg.2017.09.004

Kelly SR, Gregory FJ, Braham W, Strogen DP and Whitham AG (2015) Towards an integrated Jurassic biostratigraphy for eastern Greenland. *Volumina Jurassica* **13**, 43–64.

Khotylev OV, Balushkina NA, Vishnevskaya VS, Korobova NI, Kalmykov GA and Roslyakova AS (2019) A model of the accumulation of radiolarite layers in the Bazhenov Formation of West Siberia. *Moscow University Geology Bulletin* **74**, 206–11. doi: 10.3103/s0145875219020054

Kietzmann DA, Ambrosio AL, Suriano J, Alonso MS, Tomassini FG, Depine G and Repol D (2016) The Vaca Muerta–Quintuco system (Tithonian–Valanginian) in the Neuquén Basin, Argentina: a view from the outcrops in the Chos Malal fold and thrust belt. *American Association of Petroleum Geologists Bulletin* **100**, 743–71. doi: 10.1306/02101615121

Koevoets MJ, Abay TB, Hammer Ø and Olaussen S (2016) High-resolution organic carbon-isotope stratigraphy of the Middle Jurassic-Lower Cretaceous Agardhfjellet Formation of central Spitsbergen, Svalbard. *Palaeogeography, Palaeoclimatology, Palaeoecology* **449**, 266–74. doi: 10.1016/j.palaeo.2016.02.029

Koevoets MJ, Hammer Ø and Little CTS (2019) Palaeoecology and palaeoenvironments of the Middle Jurassic to lowermost Cretaceous Agardhfjellet Formation (Bathonian–Ryazanian), Spitsbergen, Svalbard. *Norwegian Journal of Geology* **99**, 1–24. doi: 10.17850/njg99-1-02

Koevoets MJ, Hammer Ø, Olaussen S, Senger K and Smelror M (2018a) Integrating subsurface and outcrop data of the Middle Jurassic to Lower Cretaceous Agardhfjellet Formation in central Spitsbergen. *Norwegian Journal of Geology* **98**, 1–34. doi: 10.17850/njg98-4-01

Koevoets MJ, Hurum HH and Hammer Ø (2018b) New Late Jurassic teleost remains from the Agardhfjellet Formation, Spitsbergen, Svalbard. *Norwegian Journal of Geology* **98**, 1–12. doi: 10.17850/njg98-2-01

Kosteva NN (2005) Stratigraphy of the Jurassic-Cretaceous deposits of Franz-Josef Land archipelago. *Arctic and Antarctic* **4**, 16–32 (in Russian).

Kozlova EV, Fadeeva NP, Kalmykov GA, Balushkina NS, Pronina NV, Poludetkina EN, Kostenko OV, Yurchenko AY, Borisov RS, Bychkov AY and Kalmykov AG (2015) Geochemical technique of organic matter research in deposits enrich in kerogene (the Bazhenov Formation, West Siberia). *Moscow University Geology Bulletin* **70**, 409–18. doi: 10.3103/s0145875215050075

Kulyova GV, Yanochkina ZA, Bukina TF, Ivanov AV, Baryshnikova VN, Troitskaya EA and Eryomin VN (2004) Upper Jurassic shale-bearing section of the Volga Basin (Dorsoplanites panderi zone). *Transactions of the Geological Scientific Institute of Saratov State University* **XVII**, 1–110 (in Russian).

Langrock U and Stein R (2004) Origin of marine petroleum source rocks from the Late Jurassic to Early Cretaceous Norwegian Greenland Seaway - evidence for stagnation and upwelling. *Marine and Petroleum Geology* **21**, 157–176. doi: 10.1016/j.marpetgeo.2003.11.011

Langrock U, Stein R, Lipinski M and Brumsack HJ (2003) Paleoenvironment and sea-level change in the early Cretaceous Barents Sea - implications from near-shore marine sapropels. *Geo-Marine Letters* **23**, 34–42. doi: 10.1007/s00367-003-0122-5

Leith TL, Weiss HM, Mørk A, Elvebakk G, Embry AF, Brooks PW, Stewart KR, Pchelina TM, Bro EG, Verba ML and Danyushevskaya A (1992) Mesozoic hydrocarbon source-rocks of the Arctic region. *Norwegian Petroleum Society Special Publications* **2**, 1–25. doi: 10.1016/b978-0-444-88943-0.50006-x

Lopatin NV and Yemets TP (1987) *Pyrolysis in the Oil and Gas Geochemistry*. Moscow: Nauka, 144 pp.

Lott GK, Thomas JE, Riding JB, Davey RJ and Butler N (1989) Late Ryazanian black shales in the southern North Sea basin and their lithostratigraphical significance. *Proceedings of the Yorkshire Geological Society* **47**, 321–24. doi: 10.1144/pygs.47.4.321

Magoon LB, Woodward PV, Banet Jr AC, Griscom SB and Daws TA (1987) Thermal maturity, richness, and type of organic matter of source-rock units. In *Petroleum Geology of the Arctic National Wildlife Refuge* (eds KJ Bird and LB Magoon), pp. 127–79. Northeastern Alaska: United States Geological Survey, Bulletin no. 1778.

Malone TC (1971) The relative importance of nannoplankton and netplankton as primary producers in tropical oceanic and neritic phytoplankton communities. *Limnology and Oceanography* **16**, 633–39. doi: 10.4319/lo.1971.16.4.0633

Martinez M and Dera G (2015) Orbital pacing of carbon fluxes by a ~9-My eccentricity cycle during the Mesozoic. *Proceedings of the National Academy of Sciences* **112**, 12604–9. doi: 10.1073/pnas.1419946112

Miller RG (1990) A paleoceanographic approach to the Kimmeridge clay formation. In *Deposition of Organic Facies* (ed. AY Huc), pp. 13–26. Tulsa: American Association of Petroleum Geologists, Studies in Geology no. 30.

Mohammedyasin MS, Wudie G, Anteneh ZL and Bawoke GT (2019) Paleoredox conditions of the Middle-Upper Jurassic black shales in the Blue Nile Basin, Ethiopia. *Journal of African Earth Sciences* **151**, 136–45. doi: 10.1016/j.jafrearsci.2018.12.009

Morales C, Rogov M, Wierzbowski H, Ershova V, Suan G, Adatte T, Föllmi KB, Tegelaar E, Reichart GJ, de Lange GJ and Middelburg JJ (2017) Glendonites track methane seepage in Mesozoic polar seas. *Geology* **45**, 503–6. doi: 10.1130/g38967.1

Morgans-Bell HS, Coe AL, Hesselbo SP, Jenkyns HC, Weedon GP, Marshall JE, Tyson RV and Williams CJ (2001) Integrated stratigraphy of the Kimmeridge Clay Formation (Upper Jurassic) based on exposures and boreholes in south Dorset, UK. *Geological Magazine* **138**, 511–39. doi: 10.1017/s0016756801005738

Mutterlose J, Bornemann A and Herrle JO (2005) Mesozoic calcareous nannofossils - state of the art. *Paläontologische Zeitschrift* **79**, 113–33. doi: 10.1007/BF03021757

Mutterlose J, Brumsack H, Flögel S, Hay W, Klein C, Langrock U, Lipinski M, Ricken W, Söding E, Stein R and Swientek O (2003) The Greenland–Norwegian Seaway: a key area for understanding Late Jurassic to Early Cretaceous paleoenvironments. *Paleoceanography and Paleoclimatology* **18**. doi: 10.1029/2001PA000625

Mutterlose J and Ruffell A (1999) Milankovitch-scale palaeoclimate changes in pale–dark bedding rhythms from the Early Cretaceous (Hauterivian and Barremian) of eastern England and northern Germany. *Palaeogeography, Palaeoclimatology, Palaeoecology* **154**, 133–60. doi: 10.1016/s0031-0182(99)00107-8

Nagy J, Løfaldli M and Bäckström SA (1988) Aspects of foraminiferal distribution and depositional conditions in Middle Jurassic to Early Cretaceous shales in eastern Spitsbergen. *Abhandlungen der Geologischen Bundesanstalt* **30**, 297–300.

Nikitenko BL, Knyazev VG, Peshchevitskaya EB and Glinskikh LA (2015) The upper Jurassic of the Laptev Sea: interregional correlations and paleoenvironments. *Russian Geology and Geophysics* **56**, 1173–93. doi: 10.1016/j.rgg.2015.07.008

Nikitenko BL, Pestchevitskaya EB, Lebedeva NK and Ilyina VI (2008) Micropalaeontological and palynological analyses across the Jurassic-Cretaceous boundary on Nordvik Peninsula, Northeast Siberia. *Newsletters on Stratigraphy* **42**, 181–222. doi: 10.1127/0078-0421/2008/0042-0181

Nozaki T, Kato Y and Suzuki K (2013) Late Jurassic ocean anoxic event: evidence from voluminous sulphide deposition and preservation in the Panthalassa. *Scientific Reports* **3**, Article no. 1889. doi: 10.1038/srep01889

Nunn EV, Price GD, Hart MB, Page KN and Leng MJ (2009) Isotopic signals from Callovian–Kimmeridgian (Middle–Upper Jurassic) belemnites and bulk organic carbon, Staffin Bay, Isle of Skye, Scotland. *Journal of the Geological Society* **166**, 633–41. doi: 10.1144/0016-76492008-067

Oschmann W (1988) Upper Kimmeridgian and Portlandian marine macrobenthic associations from southern England and northern France. *Facies* **18**, 49–82. doi: 10.1007/bf02536795

Oschmann W (1994) Der Kimmeridge Clay von Yorkshire als Beispiel eines fossilen Sauerstoff-kontrollierten Milieus. *Berengeria* **9**, 3–153.

Panchenko IV, Balushkina NS, Baraboshkin EYu, Vishnevskaya VS, Kalmikov GA and Shurekova OV (2015) Complexes of paleobiota in Abalak-Bazhenov deposits in the central part of Western Siberia. *Neftegazovaya Geologiya: Teoriya i Praktika* **10**. doi: 353/2070-5379/24_2015

Panchenko IV, Nemova VD, Smirnova ME and Ilyina MV (2016) Stratification and detailed correlation of Bazhenov horizon in the central part of the Western Siberia according to lithological and paleontological core analysis and well logging. *Oil and Gas Geology* **6**, 22–34 (in Russian).

Pauly S, Mutterlose J and Alsen P (2013) Depositional environments of Lower Cretaceous (Ryazanian–Barremian) sediments from Wollaston Forland and Kuhn Ø, North-East Greenland. *Bulletin of the Geological Society of Denmark* **61**, 19–36.

Peters KE, Kontorovich AE, Moldowan JM, Andrusevich VE, Huizinga BJ, Demaison GJ and Stasova OF (1993) Geochemistry of selected oils and rocks from the central portion of the West Siberian basin, Russia. *American Association of Petroleum Geologists Bulletin* **77**, 863–87. doi: 10.1306/bdff8d80-1718-11d7-8645000102c1865d

Ponomareva EV, Burshtein LM, Kontorovich AE and Kostyreva EA (2018) Organic carbon distribution in the Bazhenov Horizon rocks of the Western Siberian megabasin. *Doklady Earth Sciences* **481**, 918–21. doi: 10.1134/s1028334x18070176

Ponsaing L, Mathiesen A, Petersen HI, Bojesen-Koefoed JA, Schovsbo NH, Nytoft HP and Stemmerik L (2020) Organofacies composition of the Upper Jurassic–Lowermost Cretaceous source rocks, Danish central graben, and insight into the correlation to oils in the Valdemar field. *Marine and Petroleum Geology* **114**, 104239. doi: 10.1016/j.marpetgeo.2020.104239

Price GD and Rogov MA (2009) An isotopic appraisal of the Late Jurassic greenhouse phase in the Russian Platform. *Palaeogeography, Palaeoclimatology, Palaeoecology* **273**, 41–9. doi: 10.1016/j.palaeo.2008.11.011

Proust JN, Deconinck JF, Geyssant JR, Herbin JP and Vidier JP (1995) Sequence analytical approach to the Upper Kimmeridgian-Lower Tithonian storm-dominated ramp deposits of the Boulonnais (Northern France). A landward time-equivalent to offshore marine source rocks. *Geologische Rundschau* **84**, 255–71. doi: 10.1007/bf00260439

Rakociński M, Zatoń M, Marynowski L, Gedl P and Lehmann J (2018) Redox conditions, productivity, and volcanic input during deposition of uppermost Jurassic and Lower Cretaceous organic-rich siltstones in Spitsbergen, Norway. *Cretaceous Research* **89**, 126–47. doi: 10.1016/j.cretres.2018.10.014

Rawson PF (1973) Lower Cretaceous (Ryazanian-Barremian) marine connections and cephalopod migrations between the Tethyan and Boreal Realms. *Geological Journal*, Special Issue, **5**, 131–44.

Rees PM, Ziegler AM and Valdes PJ (2000) Jurassic phytogeography and climates: new data and model comparisons. In *Warm Climates in Earth History* (eds BT Huber, KG MacLeod and SL Wing), pp. 297–318. Cambridge: Cambridge University Press.

Remane J (1991) The Jurassic-Cretaceous boundary: problems of definition and procedure. *Cretaceous Research* **12**, 447–53. doi: 10.1016/0195-6671(91)90001-s

Remírez MN and Algeo TJ (2020) Paleosalinity determination in ancient epicontinental seas: a case study of the T-OAE in the Cleveland Basin (UK). *Earth-Science Reviews* **201**, 103072. doi: 10.1016/j.earscirev.2019.103072

Riboulleau A, Derenne S, Largeau C and Baudin F (2001) Origin of contrasting features and preservation pathways in kerogens from the Kashpir oil shales (Upper Jurassic, Russian Platform). *Organic Geochemistry* **32**, 647–65. doi: 10.1016/s0146-6380(01)00017-1

Rogov MA (2004) The Russian Platform as a key region for Volgian/Tithonian correlation: a review of the Mediterranean faunal elements and ammonite biostratigraphy of the Volgian stage. *Rivista Italiana di Paleontologia e Stratigrafia* **110**, 321–8.

Rogov MA (2010) A precise ammonite biostratigraphy through the Kimmeridgian-Volgian boundary beds in the Gorodischi section (Middle Volga area, Russia), and the base of the Volgian Stage in its type area. *Volumina Jurassica* **VIII**, 103–30.

Rogov MA (2013) Ammonites and infrazonal subdivision of the Dorsoplanites panderi Zone (Volgian Stage, Upper Jurassic) of the European part of Russia. *Doklady Earth Sciences* **451**, 803–8. doi: 10.1134/s1028334x13080059

Rogov MA (2014) Infrazonal subdivision of the Volgian Stage in its type area using ammonites and correlation of the Volgian and Tithonian Stages. In *STRATI 2013. First International Congress on Stratigraphy. At the Cutting Edge of Stratigraphy*, pp. 577–580. Springer Geology. doi: 10.1007/978-3-319-04364-7_111

Rogov MA, Baraboshkin EY, Guzhikov AY, Efimov VM, Kiselev DN, Morov VP and Gusev VV (2015) *The Jurassic-Cretaceous boundary in the Middle Volga region. Field guide to the International meeting on the Jurassic/Cretaceous boundary. September 7-13, 2015, Samara (Russia)*. Samara: Samara State Technical University, 130 pp.

Rogov M and Bizikov V (2006) New data on Middle Jurassic-Lower Cretaceous Belemnoteuthidae from Russia. What can shell tell about the animal and its mode of life. *Acta Universitatis Carolinae Geologica* **49**, 149–63.

Rogov MA and Ustinova MA (2018) High-latitude Late Jurassic nannofossils and their implication for climate and palaeogeography. *Norwegian Journal of Geology* **98**, 17–23. doi: 10.17850/njg98-1-02

Rogov M and Zakharov V (2009) Ammonite- and bivalve-based biostratigraphy and Panboreal correlation of the Volgian Stage. *Science in China Series D, Earth Sciences* **52**, 1890–909. doi: 10.1007/s11430-009-0182-0

Rogov MA, Zakharov VA and Ershova VB (2011) Detailed stratigraphy of the Jurassic–Cretaceous boundary beds of the Lena River lower reaches based on ammonites and buchiids. *Stratigraphy and Geological Correlation* **19**, 641–62. doi: 10.1134/s0869593811060050

Rogov MA, Zverkov NG, Zakharov VA and Arkhangelsky MS (2019) Marine reptiles and climates of the Jurassic and Cretaceous of Siberia. *Stratigraphy and Geological Correlation* **27**, 398–423. doi: 10.31857/s0869-592x27413-39

Rost B and Riebesell U (2004) Coccolithophores and the biological pump: responses to environmental changes. In *Coccolithophores: From Molecular Processes to Global Impact* (eds HR Thierstein and JR Young), pp. 99–125. Berlin, Heidelberg: Springer.

Ruffell AH, Price GD, Mutterlose J, Kessels K, Baraboshkin E and Gröcke DR (2002) Palaeoclimate indicators (clay minerals, calcareous nannofossils, stable isotopes) compared from two successions in the late Jurassic of the Volga Basin (SE Russia). *Geological Journal* **37**, 17–33. doi: 10.1002/gj.903

Ryzhkova SV, Burshtein LM, Ershov SV, Kazanenkov VA, Kontorovich AE, Kontorovich VA, Nekhaev AY, Nikitenko BL, Fomin MA, Shurygin BN, Beizel AL, Borisov EV, Zolotova OV, Kalinina LM and Ponomareva EV (2018) The Bazhenov Horizon of West Siberia: structure, correlation, and thickness. *Russian Geology and Geophysics* **59**, 846–63. doi: 10.1016/j.rgg.2018.07.009

Sælen G, Tyson RV, Telnæs N and Talbot MR (2000) Contrasting watermass conditions during deposition of the Whitby Mudstone (Lower Jurassic) and Kimmeridge Clay (Upper Jurassic) formations, UK. *Palaeogeography, Palaeoclimatology, Palaeoecology* **163**, 163–96. doi: 10.1016/s0031-0182(00)00150-4

Samson Y, Lepage G, Hantzpergue P, Guyader J, Saint-Germès M, Baudin F and Bignot G (1996) Révision lithostratigraphique et biostratigraphique du Kimméridgien de la région havraise (Normandie). *Géologie de la France* **3**, 3–19.

Savrda CE and Bottjer DJ (1986) Trace fossil model for reconstruction of paleo-oxygenation in bottom water. *Geology* **14**, 3–6. doi: 10.1130/0091-7613(1986)14<3:tmfrop>2.0.co;2

Scotchman IC (1991) Kerogen facies and maturity of the Kimmeridge Clay Formation in southern and eastern England. *Marine and Petroleum Geology* **8**, 278–95. doi: 10.1016/0264-8172(91)90082-c

Shchepetova EV (2009) Sedimentology of Volgian oil shale formation (Upper Jurassic, Panderi Zone) in North Russian Plate. *Bulletin of Moscow Society of Naturalists, Geological Series* **84**, 74–89 (in Russian).

Shchepetova EV and Rogov MA (2013) Organic carbon-rich horizons in the Upper Kimmeridgian of the northern part of Ulyanovsk-Saratov trough (Russian Platform): biostratigraphy, sedimentology, geochemistry. In *Jurassic System of Russia: Problems of Stratigraphy and Paleogeography, Fifth All-Russian Meeting* (eds VA Zakharov, MA Rogov and BN Shurygin), pp. 249–252. 23–27 September 2013, Tyumen. Scientific Materials. Yekaterinburg, ID IzdatNaukaServis LLC (in Russian).

Shchepetova EV and Rogov MA (2016) Organic carbon-rich shales within coarse-grained lithofacies of Jurassic–Cretaceous transition at the Russian Platform. In *Field Trip Guide and Abstracts Book, XIIth Jurassica Conference. IGCP 632 and ICS Berriasian Workshop*, pp. 95–96. 19–23 April 2016, Smolenice, Slovakia. Bratislava, Earth Science Institute, Slovak Academy of Sciences.

Shurygin BN and Dzyuba OS (2015) The Jurassic/Cretaceous boundary in northern Siberia and Boreal-Tethyan correlation of the boundary beds. *Russian Geology and Geophysics* **56**, 652–62. doi: 10.1016/j.rgg.2015.03.013

Smelror M, Mørk A, Monteil E, Rutledge D and Leereveld H (1998) The Klippfisk Formation - a new lithostratigraphic unit of Lower Cretaceous platform carbonates on the Western Barents Shelf. *Polar Research* **17**, 181–202. doi: 10.1111/j.1751-8369.1998.tb00271.x

Smelror M, Mørk A, Mørk MBE, Weiss HM and Løseth H (2001) Middle Jurassic-Lower Cretaceous transgressive-regressive sequences and facies distribution off northern Nordland and Troms, Norway. *Norwegian Petroleum Society Special Publications* **10**, 211–32. doi: 10.1016/s0928-8937(01)80015-1

Socha K and Makos M (2016) Revealing what has been overlooked – petroleum potential of the Jurassic deposits in Central Poland. In *Field Trip Guide and Abstracts Book, XIIth Jurassica Conference. IGCP 632 and ICS Berriasian Workshop*, pp. 84–85. 19–23 April 2016, Smolenice, Slovakia. Bratislava, Earth Science Institute, Slovak Academy of Sciences.

Stemmerik L, Dam G, Noe-Nygaard N, Piasecki S and Surlyk F (1998) Sequence stratigraphy of source and reservoir rocks in the Upper Permian and Jurassic of Jameson Land, East Greenland. *Geology of Greenland Survey Bulletin* **180**, 43–54.

Strachoff NM (1934) Brennschiefer der Zone Perisphinctes Panderi d'Orb. (Lithologische Übersicht). *Bulletin of Moscow Society of Naturalists, Geological Series* **XII**, 200–50 (in Russian, with abstract in German).

Suchéras-Marx B, Mattioli E, Allemand P, Giraud F, Pittet B, Plancq J and Escarguel G (2019) The colonization of the oceans by calcifying pelagic algae. *Biogeosciences* **16**, 2501–10. doi: 10.5194/bg-2018-493

Tobia FH, Al-Jaleel HS and Ahmad IN (2019) Provenance and depositional environment of the Middle-Late Jurassic shales, northern Iraq. *Geosciences Journal* 23, 747–65. doi: 10.1007/s12303-018-0072-6

Trabucho-Alexandre J, Hay WW and De Boer PL (2012) Phanerozoic environments of black shale deposition and the Wilson Cycle. *Solid Earth* **3**, 29–42. doi: 10.5194/se-3-29-2012

Tribovillard N, Bialkowski A, Tyson RV, Lallier-Vergès E, and Deconinck JF (2001) Organic facies variation in the late Kimmeridgian of the Boulonnais area (northernmost France). *Marine and Petroleum Geology* **18**, 371–89. doi: 10.1016/s0264-8172(01)00006-x

Tribovillard N, Ramdani A and Trentesaux A (2005) Controls on organic accumulation in Upper Jurassic shales of northwestern Europe as inferred from trace-metal geochemistry. In *The Deposition of Organic-Carbon-Rich Sediments: Models, Mechanisms, and Consequences* (ed. N Harris), pp. 145–64. Tulsa: Society for Sedimentary Geology, Special Publication no. 82.

Turner H, Batenburg SJ, Gale A and Gradstein F (2019) The Kimmeridge Clay Formation (Upper Jurassic–Lower Cretaceous) of the Norwegian Continental Shelf and Dorset, UK: a chemostratigraphic correlation. *Newsletters on Stratigraphy* **52**, 1–32. doi: 10.1127/nos/2018/0436

Turov AV (2000) On environmental conditions of the Upper Jurassic oil shales in the Russian Plate. *Proceedings of Higher Educational Establishments: Geology and Exploration* **3**, 9–20 (in Russian).

Tyson RV (1987) The genesis and palynofacies characteristics of marine petroleum source rocks. In *Marine Petroleum Source Rocks* (eds J Brooks and AJ Fleet), pp. 47–68. Geological Society of London, Special Publication no. 26. doi: 10.1144/gsl.sp.1987.026.01.03

Tyson RV (1995) *Sedimentary Organic Matter: Organic Facies and Paliynofacies*. London: Chapman and Hall, 615 pp.

Ulmishek GF (1993) Petroleum Geology and Resources of the West Siberian Basin, Russia. *US Geological Survey Bulletin* **2201-G**, 1–53. doi: 10.3133/b2201g

Underhill JR (1998) Jurassic. In *Petroleum Geology of the North Sea*, 4th edition (ed. KW Glennie), pp. 245–93. London: Blackwell Science Ltd.

Vakhrameyev VA (1982) *Classopollis* pollen as an indicator of Jurassic and Cretaceous climate. *International Geology Review*, **24**, 1190–6. doi: 10.1080/00206818209451058

Vishnevskaya VS, de Wever P, Baraboshkin EY, Bogdanov NA, Bragin NY, Bragina LG, Kostyuchenko AS, Lambert E, Malinovsky YM, Sedaeva KM and Zukova GA (1999) New stratigraphic and palaeogeographic data on Upper Jurassic to Cretaceous deposits from the eastern periphery of the Russian Platform (Russia). *Geodiversitas* **21**, 347–63.

Vollset J and Doré AG (1984) A revised Triassic and Jurassic lithostratigraphic nomenclature for the Norwegian North Sea. *Norwegian Petroleum Directorate Bulletin* **3**, 1–53.

Więcław D (2016) Habitat and hydrocarbon potential of the Kimmeridgian strata in the centralpart of the Polish Lowlands. *Geological Quarterly* **60**, 192–210. doi: 10.7306/gq.1260

Wierzbowski A, Hryniewicz K, Hammer Ø, Nakrem HA and Little CTS (2011) Ammonites from hydrocarbon seep carbonate bodies from the uppermost Jurassic – lowermost Cretaceous of Spitsbergen and their biostratigraphical importance. *Neues Jahrbuch für Geologie und Paläontologie, Abhandlungen* **262**, 267–88. doi: 10.1127/0077-7749/2011/0198

Wierzbowski A and Smelror M (2020) The Bajocian to Kimmeridgian (Middle to Upper Jurassic) ammonite succession at Sentralbanken High (core 7533/3-U-1), Barents Sea, and its stratigraphical and palaeobiogeographical significance. *Volumina Jurassica* **XVIII**, 1–22.

Wierzbowski A, Smelror M and Mørk A (2002) Ammonites and dinoflagellate cysts in the Upper Oxfordian and Kimmeridgian of the northeastern Norwegian Sea (Nordland VII offshore area): biostratigraphical and biogeographical significance. *Neues Jahrbuch für Geologie und Paläontologie, Abhandlungen* **226**, 145–64. doi: 10.1127/njgpa/226/2002/145

Wierzbowski A and Wierzbowski H (2019) Ammonite stratigraphy and organic matter of the Pałuki Fm. (Upper Kimmeridgian-Lower Tithonian) from the central-eastern part of the Łódź Synclinorium (Central Poland). *Volumina Jurassica* **XVII**, 49–80. doi: 10.7306/VJ.17.4

Wierzbowski H, Bajnai D, Wacker U, Rogov MA, Fiebig J and Tesakova EM (2018) Clumped isotope record of salinity variations in the Subboreal Province at the Middle–Late Jurassic transition. *Global and Planetary Change* **167**, 172–89. doi: 10.1016/j.gloplacha.2018.05.014

Wignall PB (1990) Benthic palaeoecology of the Late Jurassic Kimmeridge Clay of England. *Special Papers in Palaeontology* **43**, 1–74.

Wimbledon WA (2008) The Jurassic-Cretaceous boundary: an age-old correlative enigma. *Episodes* **31**, 423–8. doi: 10.18814/epiiugs/2008/v31i4/008

Yang R, Cao J, Hu G, Bian L, Hu K and Fu X (2017) Marine to brackish depositional environments of the Jurassic–Cretaceous Suowa Formation, Qiangtang Basin (Tibet), China. *Palaeogeography, Palaeoclimatology, Palaeoecology* **473**, 41–56. doi: 10.1016/j.palaeo.2017.02.031

Zakharov VA (2006) Tithonian–Berriasian deposition environments of the Bazhenov Formation bituminous shale in West Siberia, from paleoecological data. In *Evolution of Biosphere and Biodiversity, on the 70th Anniversary of Yu.A. Rosanov* (eds TB Leonova, AV Lopatin, SV Rozhnov, GT Ushatinskaya and AA Shevyrev). Moscow: KMK Society of Scientific Publications, pp. 552–568 (in Russian).

Zakharov VA, Baudin F, Dzyuba OS, Daux V, Zverev KV and Renard M (2005) Isotopic and faunal record of high paleotemperatures in the Kimmeridgian of Subpolar Urals. *Russian Geology and Geophysics* **46**, 3–20.

Zakharov VA, Nalnyaeva TI and Shulgina NI (1983) New data on the biostratigraphy of the Upper Jurassic and Lower Cretaceous deposits on Paksa peninsula, Anabar embayment (north of the Middle Siberia). Moscow: Nauka. *Siberian Branch of the Russian Academy of Sciences, Transactions of the Institute of Geology and Geophysics*, **528**, 56–99 (in Russian).

Zakharov VA and Rogov MA (2003) Boreal-Tethyan mollusk migrations at the Jurassic-Cretaceous boundary time and biogeographic ecotone position in the Northern Hemisphere. *Stratigraphy and Geological Correlation* **11**, 152–71.

Zakharov VA, Rogov MA, Dzyuba OS, Žák K, Košťák M, Pruner P, Skupien P, Chadima M, Mazuch M and Nikitenko BL (2014) Palaeoenvironments and palaeoceanography changes across the Jurassic/Cretaceous boundary in the Arctic realm: case study of the Nordvik section (north Siberia, Russia). *Polar Research* **33**, 19714. doi: 10.3402/polar.v33.19714

Zakharov VA, Rogov MA and Shchepetova EV (2017) Black shale events in the Late Jurassic – earliest Cretaceous of Central Russia. In *Jurassic System of Russia: Problems of Stratigraphy and Paleogeography* (eds VA Zakharov, MA Rogov and EV Shchepetova), pp. 57–63. Proceedings of 7th All-Russian Conference, 18–22 September 2017. Scientific Materials. Moscow: *Siberian Branch of the Russian Academy of Sciences, Transactions of the Institute of Geology and Geophysics* (in Russian).

Zakharov VA and Yudovny EG (1974) Conditions of sediment deposition and fauna existence in the Early Cretaceous sea of Khatanga depression. Novosibirsk: Nauka. *Siberian Branch of the Russian Academy of Sciences, Transactions of the Institute of Geology and Geophysics* **80**, 127–74 (in Russian).

Zanin YN, Zamirailova AG and Eder VG (2012) Some calcareous nannofossils from the Upper Jurassic-Lower Cretaceous Bazhenov Formation of the West Siberian marine basin, Russia. *The Open Geology Journal* **6**, 25–31. doi: 10.2174/1874262901206010025

Ziegs V, Horsfield B, Skeie JE and Rinna J (2017) Petroleum retention in the Mandal Formation, Central Graben, Norway. *Marine and Petroleum Geology* **83**, 195–214. doi: 10.1016/j.marpetgeo.2017.03.005

Zverkov NG and Efimov VM (2019) Revision of *Undorosaurus*, a mysterious Late Jurassic ichthyosaur of the Boreal Realm. *Journal of Systematic Palaeontology* **17**, 963–93. doi: 10.1080/14772019.2018.1515793